BULK AND ADSORPTION PROPERTIES OF SURFACTANT ENTRAPPED IN POLYELECTROLYTE COMPLEX NANOPARTICLES

A Thesis

by

XILONG ZHOU

Submitted to the Office of Graduate and Professional Studies of
Texas A&M University
in partial fulfillment of the requirements for the degree of

MASTER OF SCIENCE

Chair of Committee,	Jenn-Tai Liang
Committee Members,	Hisham Nasr-El-Din
	ZhengDong Cheng
Head of Department,	A. Daniel Hill

August 2016

Major Subject: Petroleum Engineering

ABSTRACT

With the wide application of nanotechnology in petroleum industry, transportation of nanoparticles in porous media has attracted a growing interest. This thesis focuses on investigating the bulk and adsorption properties of surfactant entrapped in polyelectrolyte complex (PEC) nanoparticles.

A stable surfactant entrapped in PEC system was optimized and obtained varying parameters of the preparation protocol including pH of PEI, surfactant/PEI concentrations and surfactant to PEI weight ratio. Meanwhile, the effect of different parameters on the bulk properties of PEC was investigated. In addition, surfactant entrapment efficiency (EE) of PEC was obtained using methylene blue (MB) titration method.

A TOC/TN analytical method was developed to study the static adsorption of PEC via measuring the concentration of PEI and surfactant in the PEC suspension. The prepared PEC suspension was agitated with sand grains for different time periods and analyzed using the developed TOC/TN analytical method. The TOC/TN results showed a large decrease of surfactant concentration and a small decrease of PEI concentration after shaking equilibrium. In addition, study revealed that PEC coated sand grains were more likely to adsorb surfactant than those not coated by PEC.

A hypothesis of PEC adsorption model was proposed based on the observations and proved. During the PEC adsorption test, a large amount of PECs and a small amount of free PEI will be firstly adsorbed onto the sand surface and form the first layer. Then free

surfactant will be adsorbed onto PEC/PEI coated surface due to the electrostatic reaction and the increasing surface area of the distorted nanoparticles on sand surface. Quartz crystal microbalance with dissipation (QCM-D) instrument and silicon sensor were used to confirm the proposed model by monitoring the real-time adsorption of PEC and surfactant in DI water. The silicon sensor was firstly flushed and incubated by PEC suspension, rinsed by DI water and then rinsed and incubated by surfactant solution. From frequency and dissipation data, the formation of the rigid PEC/PEI layer and the viscoelastic surfactant layer were detected. This observation agreed well with the proposed PEC adsorption model. Based on the proposed model, the wettability of rock surface may be changed by surfactant entrapped in PEC system through the amphiphilic properties of the surfactants adsorbed on the rock surface.

The effect of salinity and sand type on PEC adsorption was investigated, too. PEC adsorbed to sand surface faster in electrolyte solution than in DI water which can be explained by the Derjaguin-Landau-Verwey-Overbeek (DLVO) theory. In addition, in DI water a faster adsorption of PEC on carbonate than sandstone was observed.

ACKNOWLEDGEMENTS

I would like to thank my committee chair, Dr. Liang, for his patient guidance about my research and thesis. Without his help, it is impossible for me finish this research. Also, I would say thank you for my committee members, Dr. Nasr-El-Din, Dr. Cheng for their guidance and support.

Next I would like to thank three research staffs in our Group, Ying-Ying Lin, Jiajia Cai, and Huili Guan. Thank you for helping me come over lots of difficulties during the experiment and giving me many meaningful academic suggestions.

Moreover, I would also like to say thank you to all my friends in this group, Shawn, Corbin, Joshua and Dinara, who helped me a lot in many aspects. Meanwhile, thanks go to all the staffs in the Writing Center of Texas A&M University about optimizing my expressions and grammar in this thesis.

NOMENCALTURE

AFM	Atomic-force Microscopy
CMC	Critical micelle concentration
CAC	Critical aggregation concentration
DLVO	Derjaguin-Landau-Verwey-Overbeek
EE	Entrapment Efficiency
HLB	Hydrophilic-lipophilic balance
IC	Inorganic Carbon
IFT	Interfacial Tension
MB	Methylene Blue
NPs	Nanoparticles
PEC	Polyelectrolyte Complex
PEI	Polyethylenimine
QCM-D	Quartz Crystal Microbalance with Dissipation
TC	Total Carbon
TN	Total Nitrogen
TOC	Total Organic Carbon

TABLE OF CONTENTS

Page

LIST OF FIGURES

Page

LIST OF TABLES

Page

CHAPTER I

INTRODUCTION

Nanotechnology has gained lots of attention in petroleum industry because of its benefits from formation evaluation, drilling, completion (Hoelscher et al. 2012, Santra et al. 2012) to reservoir characterization (Agenet et al. 2012, Bennetzen et al. 2014) and enhanced oil recovery (EOR) (Ogolo et al. 2012). Hoelscher et al. (2012) found that water based drilling fluid with nanoparticles had the potential to plug the nanometer-sized pores in shale formation which further shut off drilling fluid loss. Santra et al. (2012) discussed the application of carbon nanotube, nanosilica, and nanoalumina in well completion and compared them with typical cementing accelerator. In addition, since NPs are resistant to harsh environment and are small in size, they can penetrate deeper into the formation easily. The significant changes of NPs in optical, magnetic and electrical properties make them ideal candidates of imaging agents (Bennetzen et al. 2014). Agenet et al. (2012) developed a new family of tracer based on fluorescent silica colloids for in-situ real-time monitoring of fluid flow distribution. Moreover, EOR is another potential field for nanotechnology. Ogolo et al. (2012) tested the capability of using eight different types of nanoparticles for EOR purposes. His results indicated that aluminum oxide nanoparticle was able to reduce oil viscosity whereas silicon oxide nanoparticle was capable of changing the wettability of rock surface. Onyekonwu et al. (2010) observed that polysilicon nanoparticles played a role in changing rock wettability and reducing interfacial tension between oil and water. Ragab et al. (2015) found that the recovery factor was larger when smaller nanoparticles were used. Studies were extended focusing on the

retention and transportation of NPs in porous media as well. Hendraningrat et al. (2012) observed the retention of hydrophilic silica nanoparticles in glass micromodel, made of 2-dimensional pore structure etched onto surface of a flat glass plate and covered by another flat glass plate. Yu et al. (2010) stated that the existence of salt ions in the system dramatically increased NPs retention which can be explained by DLVO theory. The application of polyelectrolyte complex was studied as well. Cordova et al. (2008) developed Cr loaded PECs and proved their effectiveness of entrapping and delivering Cr (III) with good colloidal stability. The Cr loaded PECs were capable of delaying gelation time of HPAM by 7 days at 40 ℃. This technique can be used for in-depth placement of polymer gels for water shutoff and conformance control. Gao et al. (2013) studied the interfacial properties of surfactant entrapping PEC by measuring the surface tension and interfacial microrheology data. They observed the interface triggered disassembly of PEC into their components and proposed that PEC may be used for delivery and delayed release of surfactants at the fluid/fluid interfaces. Gao (2014) also studied the adsorption of PEC using QCM-D on gold and silicon sensors as well as discussed the effect of different ions on PEC adsorption. However, only mass and thickness of adsorbed PEC on sensors measured by QCM-D were studied. PEC adsorption on real sand grains and PEC adsorbing mechanism were not fully investigated.

The objectives of this thesis include 1) obtaining a stable surfactant entrapped in PEC system and 2) developing an analytical method, which can be used to measure the concentrations of surfactant and polyethylenimnie in PEC suspension, in order to analyze the adsorption of PEC on real sand grain surface and study the PEC adsorption mechanism.

CHAPTER II

LITERATURE REVIEW

2.1 Surfactant entrapped in PEC

2.1.1 Surfactant

Surfactants are widely used in petroleum industry and applied to many aspects including drilling fluid, oil well injection, oil transportation and processing (L.Schramm 2000). Surfactants are mostly amphiphilic organic compounds, consisting of hydrophilic heads and hydrophobic tails. In aqueous solution, the hydrophilic head of a surfactant diffuses in the water and the hydrophobic tail extends out of water phase to oil; yet in organic solution the condition is opposite (see Fig. 1 for surfactant structure in organic and aqueous solution).

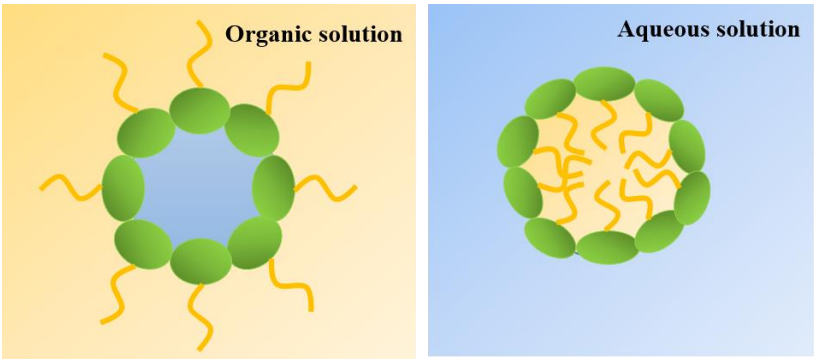

Figure 1 Chemical structure of a surfactant molecule in organic solution (left) and aqueous solution (right)

The hydrophobic tails of different surfactants are fairly similar which made up of long hydrocarbon chains. Surfactants are thus mostly characterized by head groups. Generally, surfactants are divided into four types based on the charge of head groups: non-ionic,

anionic, cationic and zwitterionic surfactants. Critical micelle concentration (CMC) is an important characteristic of a surfactant. Before surfactant concentration reaches CMC, surfactants do not form micelles and surface tension of solution changes strongly with the concentration of surfactant. After the surfactant concentration reaches its CMC, surfactants begin to suspend in aqueous solution and form micelles where hydrophobic tails act as the core of the aggregate and hydrophilic heads coat the micelle in contact with outside water. The shape of micelles depends on the hydrophilic-lipophilic balance (HLB), which is the balance of the hydrophilic heads and the hydrophobic tails. Surfactant with an HLB value of 0 is completely hydrophobic and with an HLB value of 20 is completely hydrophilic.

Surfactants are widely applied to improve oil recovery. On one hand, surfactant can lower the interfacial tension (IFT) between oil and water, and motivate the formation of emulsion to mobilize the trapped oil in porous media (Levitt et al. 2009, Sandersen 2012). On the other hand, the adsorption of surfactant on rock can control and change the wettability of rock surface. Somasundaran et al. (2006) proposed that during the surfactant adsorption process wettability of rock surface changed from water-wet to oil-wet to less oil-wet. Therefore, the dual function of IFT reduction and wettability alteration achieve higher oil recovery (Wang et al. 2011).

2.1.2 Polyelectrolyte

Polyelectrolytes are polymers containing electrolyte groups which make polymers charged in aqueous solution. Polyelectrolytes are subdivided into two types: strong

polyelectrolytes and weak polyelectrolytes. The charges of strong polyelectrolytes appear to be permanent unless the pH of the solution is extremely high or low. However, the charges of weak polyelectrolytes depend on the solution pH because weak polyelectrolytes are partially dissociated at intermediate pH. In addition to pH of the solution, the ionic strength of the solution also has a great impact on the charges of polyelectrolytes. For example, highly charged polyelectrolytes, e.g. DNA, only exist in the solution when ionic strength is low (Nylander et al. 2006).

Polyethylenimine (PEI) is widely used in medical and biological industry as gene delivery and transfection reagent because the strong positive charge on its surface make it interact with negatively charged components of the cell membranes easily (Boussif et al. 1995). The chemical structure of PEI is shown in Fig. 2.

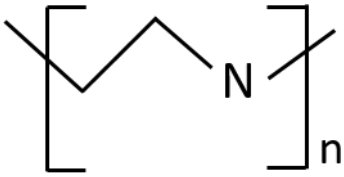

Figure 2 Chemical structure of PEI

In gene transfer technique, Rezvani Amin et al. (2013) investigated the effect of pH on the transfection efficiency of PEI. PEI is a weak polyelectrolyte, which contains lots of repeated amine groups. The amine groups are protonated (NH_3^+) at neutral pH environment and deprotonated (NH_2) at high pH environment. Thus, PEI will become neutrally charged in the high pH environment and positively charged in neutral pH environment.

2.1.3 Surfactant entrapped in PEC

PEC is the associated complex formed by oppositely charged components. PEC has wide potential applications in many aspects including drug delivery, waste water treatment, mining, paper production, cosmetics and detergent (Lankalapalli et al. 2009). There are many types of PECs including polyelectrolyte-polyelectrolyte, polyelectrolyte-surfactant, polyelectrolyte-drug, etc. Surfactant entrapped in PEC is formed by the combination of cationic polyelectrolyte and anionic surfactant. An example of an anionic surfactant entrapped in PEC is shown in Fig. 3.

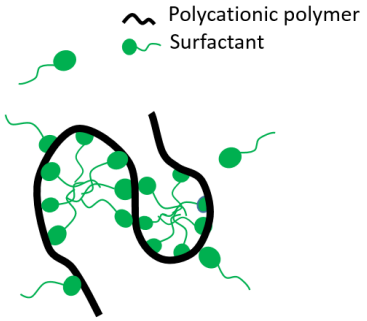

Figure 3 Structure of surfactant entrapped in PEC

The association between anionic surfactant and cationic polyelectrolyte is mainly driven by electrostatic and hydrophobic force. The addition of electrolyte tends to partially screen out the electrostatic interaction and control the binding process, further influencing the micellization equilibrium and morphology of PEC (Solomatin et al. 2003). Bain et al. (2010) and Nylander et al. (2006) proposed that the cooperative binding of surfactant to polyelectrolyte occurred above the surfactant critical aggregation concentration (CAC), which was lower than CMC of pure surfactant. Furthermore, the release of counter ions

resulted in an entropy gain, leading to the hydrophobic force between the oppositely charged surfactant and polyelectrolyte (Ondaral et al. 2010, Gao 2014).

The characteristics of PEC are influenced by many factors including nature of the surfactant, mixing order, surfactant/polyelectrolyte concentrations, and ratio of surfactant to polyelectrolyte. Müller et al. (2005) obtained PEC with needlelike particle shape and hemispherical particle shape using different molecules. Naderi et al. (2005) found that the mixing order had an effect on the characteristics of PEC. Their results showed that stable PEC was obtained when surfactant solution was added to polyelectrolyte solution. Moreover, the effect of mixing speed was discussed by Mezei et al. (2007). They proved that zeta potential did not depend on the mixing speed whereas PEC with larger particle size was obtained by slowly mixing (Mezei et al. 2008).

2.2 Adsorption characteristics of surfactants and nanoparticles

2.2.1 Adsorption characteristics of surfactants

Adsorption of surfactants have been studied by many researchers because the retention of surfactants in porous media increases the cost of EOR procedure significantly. Adsorption process of surfactant is described as the transfer of surfactant molecules from solution phase to the solid surface (Paria et al. 2004). The adsorption forces are mainly summarized as follows: 1) ion exchange: counter ions adsorbed onto the adsorbents are replaced by similar charged ions from surfactant; 2) ion pair: surfactant molecules are adsorbed on the oppositely charged adsorbents by electrostatic interaction; 3) hydrophobic bonding: a hydrophobic group of adsorbed molecule attract a molecule present in the solution; 4)

hydrogen bonding formation: a formation of hydrogen bonding between adsorbates and adsorbents (Paria et al. 2004). The adsorption force of surfactant on solid/liquid interface depend on three factors (Rosen 2004): the characteristics of solid and surfactant as well as the adsorption environment.

Many studies were conducted to study the charge of rock surface. Robertson et al. (1997) proposed that pH and ionic strength have effects on the charge of mineral. Silicon oxide is the main component of earth and Berea sandstone. The principle of how silica oxide acquire a charge in different pH environment is shown as follows. Sandstone is negatively charged in the neutral pH environment (Paria et al. 2004).

$$SiOH + H^+ = SiOH_2^+$$

$$SiOH + OH^- = SiO^- + H_2O$$

In addition to sandstone, dolomite and calcite were studied as well. Pokrovsky et al. (1999) proposed that the surface charge of dolomite is a function of pH and ionic strength. They built up a surface complexation model to describe the metal and ligand adsorbed onto dolomite surface. Li et al. (2014) observed the change of calcite surface charge as a function of ionic strength in NaCl and Na_2SO_4 solution, which was predicted by the DLVO theory.

The DLVO theory is named after Derjaguin, Landau, Verwey, and Overbeek. It mainly describes the stability of colloidal suspension and the balance between the electrostatic force and the van der Waals force. When two particles are approaching each other, the

repulsion force tends to play a leading role and the energy barrier prevents the two particles adhering together, further stabilizing the colloidal system (See Fig. 4 for the DLVO theory). The energy barrier is affected by zeta potential of particle surface and the electrolyte in the system (Ghosh). As zeta potential becomes higher, the energy barrier gets larger. In addition, the increasing concentration of electrolyte reduces the energy barrier due to the decreasing extension of double layer. The concentration of electrolyte below which the energy barrier is zero is defined as the critical aggregation concentration (Ghosh). The colloid particles are unstable at this electrolyte concentration and coagulate rapidly.

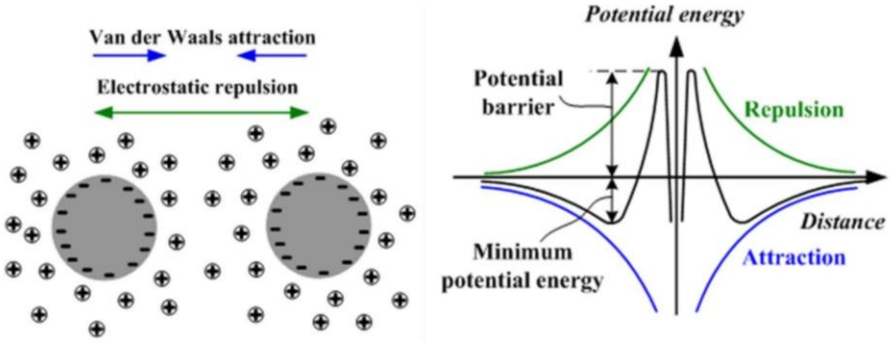

Figure 4 The DLVO theory (Soft Matter Wiki)

Many researchers investigated the adsorption characteristics of EOR surfactant. Kwok et al. (1993) studied the adsorption of non-ionic EOR surfactant on Berea sandstone and discussed the effect of sodium chloride concentration, pH, and injection flow rate on surfactant adsorption. Nevskaia et al. (1998) and Kwok et al. (1993) pointed out that the addition of electrolyte increased the adsorption of anionic and nonionic surfactants on a similarly charged surface. Biswas et al. (1998) compared the adsorption of three types of

surfactants on silica surface. Their observation showed that the order of adsorption rate was cationic surfactant > nonionic surfactant > anionic surfactant. The effect of alkaline on adsorption was illustrated by Lv et al. (2011). They proved that the presence of alkaline dramatically decreased the adsorption of both anionic and amphoteric surfactants onto the kaolinite. Gao et al. (2012) utilized TOC-L instrument to study the surfactant adsorption on sandstones and her tests showed that the retention of lab synthesized Gemini surfactant on sandstone was lower than conventional EOR surfactant.

2.2.2 Adsorption characteristics of nanoparticles

Many people studied the adsorption of different nanoparticles (e.g. silica, carbon, alumina and PEC) on different surfaces (e.g. silica, sandstone and dolomite). Yu et al. (2010) studied the transportation of carbon NPs in dolomite and Berea sandstone. Their results suggested that the surface charge played a main role in NP adsorption, and with the increase of ionic strength more NPs deposited on rock surface. They also stated that the formation of salt bridge (shown in Fig.5) between negatively charged NPs, Ca^{2+}, and Mg^{2+} influenced the transportation of NPs.

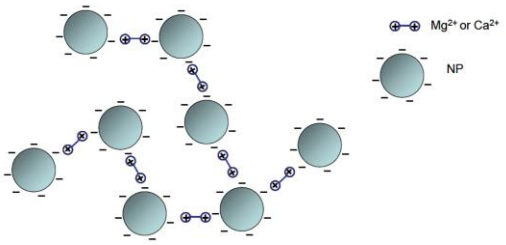

Figure 5 Divalent ion-induced salt bridge between NPs (Yu et al. 2010)

Brenner et al. (2012) found that the adsorption of positively charged maghemite nanoparticles on negatively charged silica surface was stronger and more stable than negatively charged gold nanoparticles. They thus concluded that the electrostatic interaction was the major driving force for adsorption. Li et al. (2014) studied the adsorption of silica nanoparticles on calcium carbonate immersed in different electrolyte solutions. They observed that the retention of silica nanoparticles in NaCl solution was more significant which was explained by DLVO theory. They also concluded that the retention of nanoparticles was primarily influenced by surface charge. The study of PEC adsorption was conducted by several researches. Reihs et al. (2003) studied the adsorption of PEC particles on silica surface and they proposed that the influencing factors of PEC adsorption included surface pretreatment, polyanion, pH, and centrifugation. The adsorption of centrifuged and refined PEC on pre-modified silicon surface was stronger compared to the uncentrifuged PEC (Reihs et al. 2004). They thought that the excess smaller PEI adsorbed on the negatively charged silica surface prior to larger PEC particles, which further prevented the adsorption of PEC. Using Quartz Crystal Microbalance with Dissipation (QCM-D) and Atomic-force Microscopy (AFM), Ondaral compared the adsorption process of two types of PECs with higher and lower molecule mass. They also proposed the surface-induced rearrangement due to the migration of polyelectrolytes from one PEC to another PEC (Ondaral et al. 2010). Yanez Arteta et al. (2013) observed a significant difference between the adsorption of premixed dendrimers/surfactant and the preadsorbed dendrimers/surfactant. Gao (2014) studied the adsorption of surfactant

entrapping PEC on gold and silicon sensors by QCM-D and discussed the effect of different ions on PEC adsorption.

To our best knowledge, although many studies about the adsorption of different nanoparticles on different surfaces have been done, the adsorption of EOR surfactant entrapped in PEC nanoparticles on real rock grains has not been fully investigated. Based on the theories and analytical methods proposed by previous researchers, this thesis focuses on studying the adsorption of a stable EOR surfactant entrapped in PEC system on real sand grains in DI water and in synthetic brine.

CHAPTER III

MATERIALS AND APPARATUS

3.1 Chemicals

DI water system was obtained from the EMD Millipore Corporation. EOR sulfate surfactant (referred to as sulfate surfactant for simplicity) was provided by the Shell Oil Company. Sodium dodecyl sulfate, SDS (MW: 288.38 g/mol) and sodium carbonate (Na_2CO_3) were obtained from the Fisher Scientific. Branched polyethylenimine, PEI (average MW: 25,000 g/mol by LS, average Mn: 10,000 g/mol by GPC) was purchased from the ALDRICH company. Chloromethane ($CHCl_3$) was obtained from the Acros Organics. Sodium chloride (NaCl) was purchased from the BDH. Potassium chloride (KCl), calcium chloride dehydrate ($CaCl_2•2H_2O$), magnesium chloride hexahydrate ($MgCl_2•6H_2O$) and sodium sulfate (Na_2SO_4) were obtained from the Fisher Chemical Company. Sodium chloride was purchased from the VWR. All other chemicals used in these experiments were purchased from the Sigma-Aldrich, including sodium borate ($Na_2B_4O_7$), methylene blue, MB ($C_{16}H_{18}N_3SCl$), hyamine ($C_{27}H_{42}ClNO_2$), hydrochloric acid (12M, 37%), dichloroform (CH_2Cl_2), potassium hydrogen phthalate ($C_8H_5KO_4$), sodium hydrogen carbonate sand($NaHCO_3$), sodium carbonate sand(Na_2CO_3) and potassium nitrate (KNO_3).

3.2 Apparatus

3.2.1 UV-Vis instrument

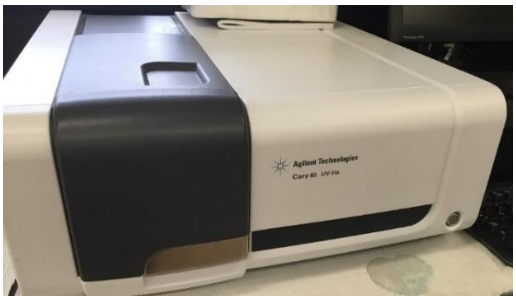

Figure 6 Cary 60 UV-vis spectrophotometer instrument

Cary 60 UV-Vis spectrophotometer instrument (Shown in Fig. 6) purchased from the Agilent Technologies was used to measure the surfactant concentration in supernatant. The absorbance of the light, obtained from the ratio of the intensities of light before and after passing through the analytes, is transformed to analyte concentration by the standard calibration curve.

3.2.2 NanoBrook Omni instrument

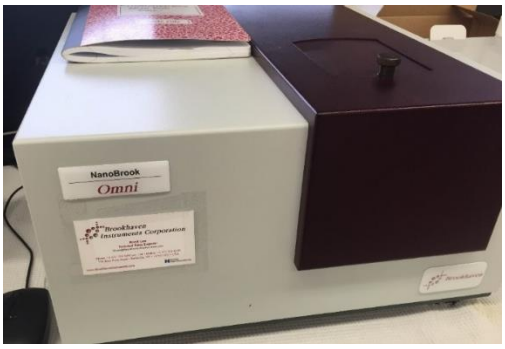

Figure 7 NanoBrook Omni instrument

NanoBrook Omni (Shown in Fig. 7) from Brookhaven Instrument Corporation was used to measure particle size and zeta potential of PEC. The measurement of particle size is based on the dynamic light scattering technique (DLS). The particle tends to scatter light when lighted by laser. Besides, the intensity of scattering light fluctuates over time. The analysis of the intensity and fluctuation of the light yields particle size. The detectable range of particle size of this instrument is from 0.3 nm to 10 um (Brookhaven Instrument corporation). Phase Analysis Light Scattering (PALS) technique is the principle of analyzing zeta potential of PEC. The shift of phase, defined as frequency multiplied by time, is measured in the scattered light caused by particles movement in an applied electric field. The measured phase shift is processed to determine the electrophoretic mobility of PEC (Malvern Instrument). The detectable range of zeta potential of this instrument is from -500 mv to 500 mv (Brookhaven Instrument corporation).

3.2.3 TOC-L instrument

Figure 8 TOC-L and TNM-L units (left) and ASI unit (right) of TOC-L instrument

TOC-L instrument (Shown in Fig. 8) purchased from the Shimadzu Company was used to quantitatively measure the carbon and nitrogen concentration in the solution. TOC-L instrument is composed of three parts: TOC-L unit, function of which is to detect total carbon (TC) and inorganic carbon (IC) concentration; TNM-L unit, which detects the concentration of total nitrogen (TN); and ASI unit, which is used to control the injection volume and injection speed of the solution.

680℃ combustion catalytic oxidization method is adopted to measure total organic carbon (TOC) concentration (Shimadzu Company July, 2013). In TC measurement, the sample is delivered into a combustion tube. By heating them to 680℃, the organic compounds can be efficiently oxidized in oxygen-rich environment in the combustion tubes filled with platinum catalyst. Then the generated carbon dioxide will be detected by an infrared gas analyzer (NDIR). The concentration of TC is obtained based on the formed peak and calibration curve. In IC concentration measurement, the sample is acidized using small amount of hydrochloric acid, which converts inorganic carbon to carbon dioxide. The carbon dioxide is detected by NDIR to generate a peak, which is then transformed to IC concentration. Total organic carbon (TOC) concentration is then obtained by subtracting IC concentration from TC concentration. The schematic of the principle of measuring TOC concentration is shown in Fig.9.

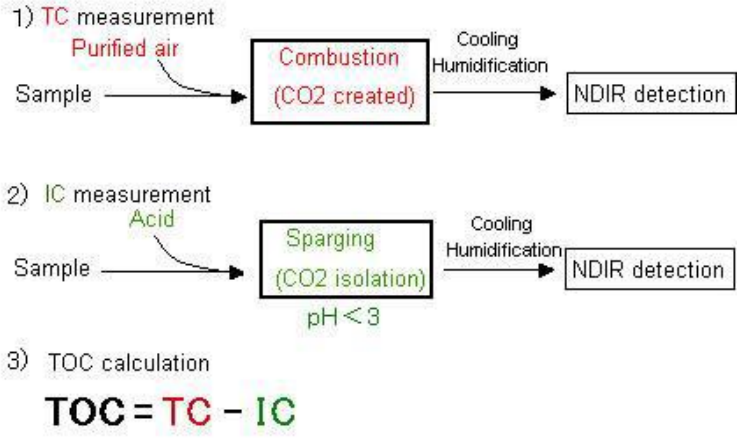

Figure 9 Principle of TOC measurement (Shimadzu Company July, 2013)

The function of TNM-L unit is to measure TN concentration in the solution. In TN measurement, the sample is introduced to combustion tube with furnace temperature 720℃, where total nitrogen is decomposed to nitrogen monoxide and nitrogen dioxide. An excited state of nitrogen dioxide is formed by the reaction between generated nitrogen species and ozone. Once these excited nitrogen dioxide return to ground state light energy will be emitted. Then, total nitrogen is obtained using a chemiluminescence detector by detecting the emitted light energy (Karnel R. Walker).

3.2.4 QCM-D instrument

Quartz Crystal Microbalance with Dissipation (QCM-D) has emerged as very sensitive technique based on its piezoelectric and electromechanical oscillator principle. It enables a real-time surface monitoring of both mass and structural properties of multiple layers. QCM-D instrument (See Fig. 10) purchased from Q-sense was utilized to monitor the real-time adsorption of samples.

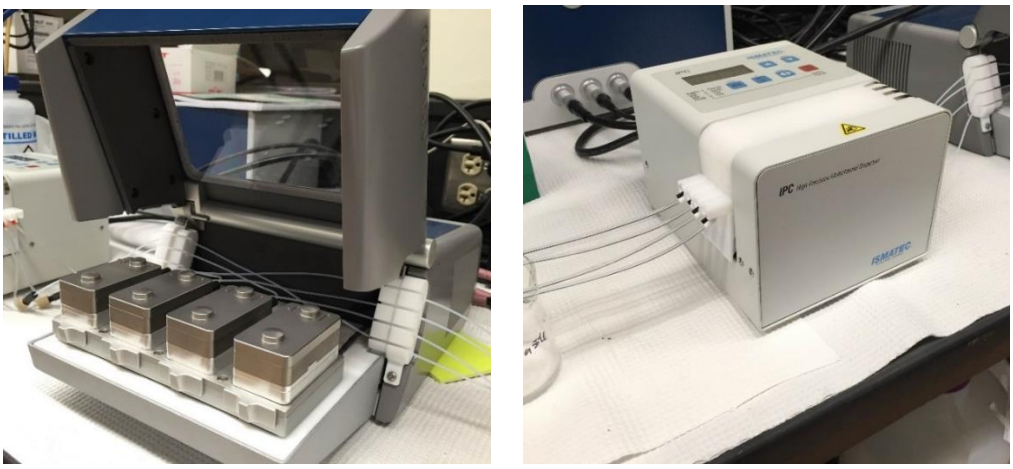

Figure 10 Flow modules (left) and pump unit (right) of QCM-D instrument

The heart of QCM-D lies in the measurements of two variables: frequency shift (Δf) and energy dissipation shift (ΔD). Δf reflects the mass change of the adsorbed materials on sensor and ΔD yields the properties of the film. The quartz crystal oscillates at its resonance frequency when voltage is applied (Q-Sense Company). When materials are adsorbed onto the sensor, Δf will decrease. The relationship of mass change (Δm) and Δf follows the Sauerbrey equation (Q-Sense Company , Sean X. Liu August, 2009)

$$\Delta m = -C * \Delta f$$

Where C is the mass sensitivity constant (=17.7 ng/cm^2). This equation is valid for evenly distributed, rigid, and sufficiently thin adsorbed layers.

Structural properties are measured as the shift in dissipation (damping) of the oscillating crystal. Dissipation is determined as the time it takes for the oscillation to stop when the power is disconnected. It is defined as the ratio of energy lost per one oscillation cycle to the total energy stored in the oscillator.

$$D = E_{lost}/2\pi E_{stored}$$

Where E_{lost} is the energy lost during one oscillation cycle and $E_{stored}$is the total energy stored in the oscillating system. When dissipation value is large enough (D shift larger than 5% of F shifts or there exists significant D difference between different overtones), the adsorption film is treated as viscoelastic film and Voigt Model is supposed to be used. Kevin-Voigt model is described as:

$$G^* = G' + iG''$$

Where $G^*$is complex shear modulus, $G'$is the storage modulus, and $G''$is the loss modulus.

CHAPTER IV

EXPERIMENTS AND METHODS

4.1 Bulk properties of PEC

4.1.1 Preparation of PEC

To make surfactant entrapped in PEC, surfactant solution was rapidly added to the vortex of PEI solution stirred at 1,200 rpm using syringe. The whole operation was performed at room temperature. After the addition of surfactant solution, the mixture was allowed to stir for another one minute. Schematic of PEC preparation process is shown in Fig. 11.

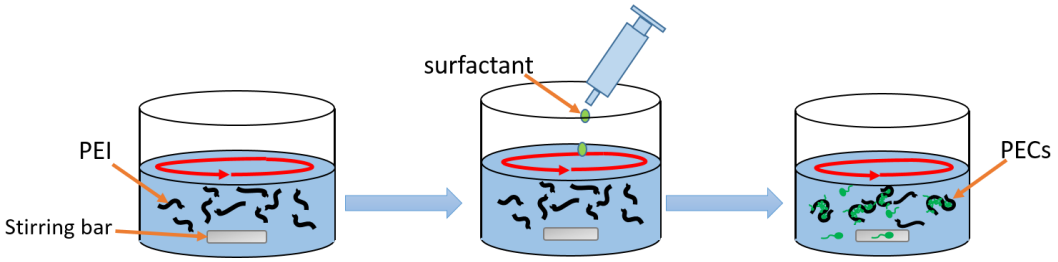

Figure 11 Preparation process of surfactant entrapped in PEC

4.1.2 Characterization of PEC

4.1.2.1 Particle size and zeta potential of PEC

The characteristics of PEC largely depend on the parameters of PEC preparation protocol including surfactant/PEI concentrations, surfactant to PEI weight ratio, pH of PEI, mixing order, and mixing speed. NanoBrook Omni was used to measure two important parameters of PEC, which are particle size and zeta potential. All the measurements were conducted at 25℃. To measure particle size, 4 drops of prepared PEC suspension was added into 3

ml DI water in the cuvette. To measure zeta potential, 8 drops of PEC suspension and 1.25 ml of 1 mM KCl solution were added into the cuvette.

4.1.2.2 Optimization of PEC

Surfactant/PEI concentrations, surfactant to PEI weight ratio, and pH of PEI are the varying parameters of PEC preparation protocol in this research. At fixed surfactant to PEI weight ratio and PEI pH, different concentrations of surfactant solutions were mixed with different concentrations of PEI solutions to investigate the effect of concentration on PEC characteristics. The influence of weight ratio was discussed by varying surfactant to PEI weight ratio at fixed PEI pH and surfactant/PEI concentrations. Moreover, pH of PEI was changed to investigate the effect of PEI pH on the characteristics of PEC at fixed surfactant/PEI concentrations and weight ratio. Based on the optimization results (discussed in Chapter 5), a stable PEC system made from the preparation protocol of 1% sulfate surfactant: 1% PEI (pH=7) = 1:1 was selected for further studies.

4.1.2.3 Stability test of PEC

The stability of prepared PEC was tested in different concentrations of sodium chloride solutions (2.5%, 5%, 7.5%, 10%, and 15%). In addition to the appearance observation of PEC in sodium chloride solution, particle size and zeta potential of PEC were measured after mixed with different sodium chloride solutions.

4.1.2.4 PEC surfactant EE measurement

Prepared PEC suspension contains free surfactant, free PEI and surfactant entrapped in PEC. Since the functional component surfactants are delivered by PEC in porous rock

media, it is important to know how much surfactants are entrapped by polyelectrolytes and how much free surfactants are present in PEC suspension before studying the adsorption of PEC. To separate PEC, free PEI, and free surfactant, prepared PEC suspension was centrifuged at 14,800 rpm for 90 minutes. Centrifuged PEC suspension in a microcentrifuge tube is shown in Fig. 12.

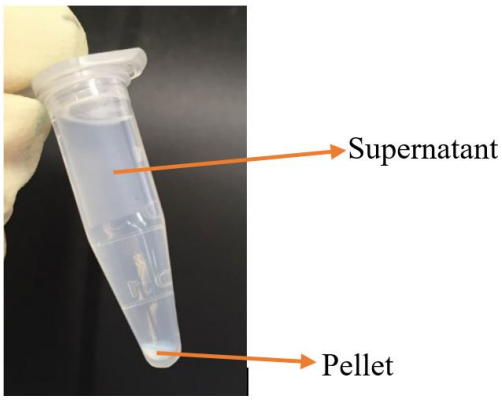

Figure 12 PEC suspension after centrifugation

The pellet in the bottom of the microcentrifuge tube is the precipitated PEC. The supernatant, consisting of free surfactant, free PEI, and a small amount of unprecipitated PEC, was aspirated for PEC surfactant EE measurement.

Surfactant EE of PEC reflects the percentage of surfactants entrapped by polyelectrolytes, which is defined as the ratio of surfactant concentration entrapped by polyelectrolyte to the initial surfactant concentration in the solution before the formation of PEC.

$$EE\ (\%) = \frac{(C_{initial} - C_{supernatant})}{C_{initial}} \times 100\% \quad (1)$$

Where $C_{initial}$ represents the initial surfactant concentration before the formation of PEC, $C_{supernatant}$ refers to surfactant concentration in the supernatant after centrifugation. UV spectroscopy and titration methods were discussed to measure surfactant EE of PEC.

4.1.2.4.1 Methylene blue UV spectroscopy method for PEC surfactant EE measurement

Jurado et al. (2006) put forward a simplified spectrophotometric method for determining anionic surfactant concentration based on the formation of surfactant-methylene blue (AS-MB) ion pair. The pair can be detected by the UV spectrophotometer at wavelength of 650 nm. The intensities of UV absorbance of five standard surfactant solutions were firstly measured to build up a standard calibration curve. Then, the supernatant from the centrifuged PEC was diluted to make it within the range of the calibration curve. 5ml of diluted supernatant was transferred to a vial and mixed with 100ul of stabilized MB (0.1g of MB dissolved in 100ml of 10mM borate buffer, pH 5−6), 4ml of methylene chloride and 200ul of 50mM sodium tetraborate buffered at pH 10.5. After one minute of vigorous shaking, the mixture was allowed to repose for five minutes. Two layers, upper aqueous layer and lower organic layer, appeared in the vial after the repose. The concentration of surfactant in the supernatant was calculated by measuring the UV absorbance of AS-MB pair at UV wavelength 650 nm. The procedure of MB UV spectroscopy method is shown in Fig. 13.

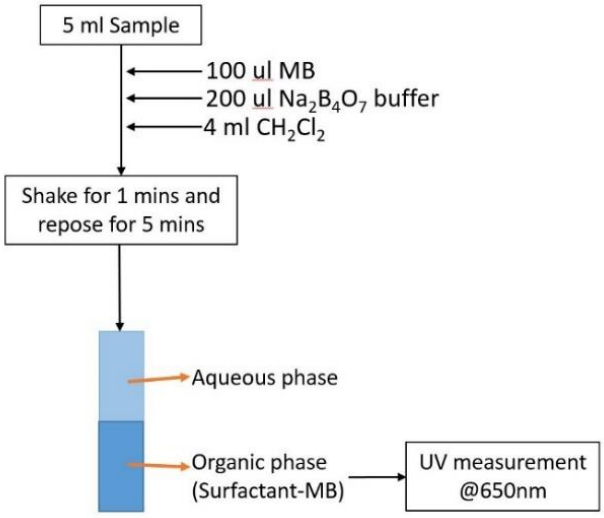

Figure 13 Schematic of MB UV spectroscopy method

4.1.2.4.2 Methylene blue titration method for PEC surfactant EE measurement

The titration method was firstly developed by S.R.Epton (December, 6, 1947). In his experiment, 10 ml of alkyl sulfate was firstly added into a vial and 25 ml of color indicator containing 0.003% MB, 1.2% sulfuric acid and 5% sodium sulfate was mixed with the analyte, followed by 15ml of chloroform. Solution of cetyl pyridinium bromide with concentration 0.004 M was used as titrant. The point where the two phases showed the same color was considered as the ending point of this titration method. The concentration of analyte was calculated from the amount of titrant spent in the experiment.

Based on Epton's method, methylene blue (MB) titration method was modified and used for PEC surfactant EE measurement. 2ml of PEC supernatant was pipetted into a 20ml vial. 2ml of DI water and 50ul of stabilized MB (0.1 g of methylene blue dissolved in 100 mL of 10 mM borate buffer, pH 7-7.5) were added, followed by 5ml of chloroform. 4mM cationic hyamine was used as titrant and added drop wise to the mixture. After each small

addition of titrant, the mixture was shaken and kept still for one minute. Before titration, the blue color concentrated in the lower organic layer because of the formation of surfactant-MB pair. As titration proceeded, surfactant and MB molecules separated from surfactant-MB pair due to the formation of surfactant-hyamine pair. Then the separated MB molecules transfer to the upper aqueous layer, leading to a blue color transfer from the lower organic layer to the upper aqueous layer. Finally, titration reached the ending point when both upper and lower layers showed the equivalent blue color. See Fig.14 for the principle of MB titration method.

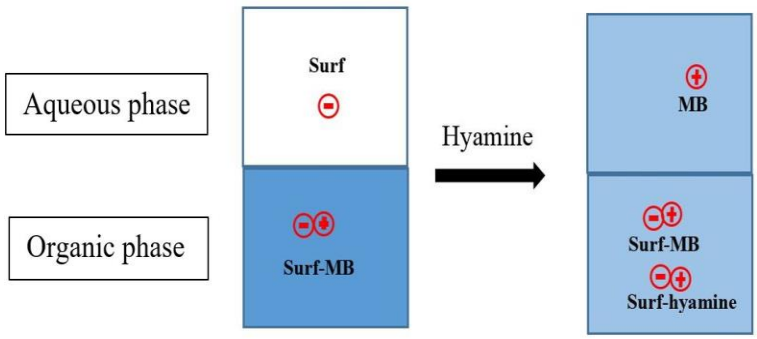

Figure 14 Schematic of MB titration method

Based on the hyamine spent in MB titration experiment, sulfate surfactant concentration was calculated using the following equation:

$$C_{surfactant}\ (\%) = \frac{V_{hyamine}\ (ml) \times 4 \times 10^{-6} M \times M_{surfactant}}{2\ ml} \times 100\% \qquad (2)$$

Where $C_{surfactant}$ represents the surfactant concentration, $V_{hyamine}$ is the volume of hyamine spent during the titration process, $M_{surfactant}$ refers to the molecular weight of

sulfate surfactant, which is 700g/mol, $4 \times 10^{-6}\ M$ refers to the concentration of hyamine, and 2ml in the denominator of equation (2) represents the initial volume of sulfate surfactant solution.

4.1.3 Surfactant release from PEC test

Surfactant entrapped in PEC is formed by the electrostatic force between cationic polyelectrolyte and anionic surfactant. PEI is a weak polyelectrolyte, so the charge of PEI largely depends on the pH of PEI. PEI is neutrally charged in high pH solution and strongly positively charged when pH is close to 7. Therefore, in order to release surfactant from PEC, electrostatic force between PEI and surfactant can be decreased through changing the pH of PEI. Sodium carbonate powders were thus added to PEC suspension to make 1% of sodium carbonate in PEC suspension. Then methylene blue titration method was followed to confirm the release of surfactants from PEC.

4.2 Adsorption study of PEC

4.2.1 Static adsorption study

4.2.1.1 Static adsorption test

Static adsorption of sulfate EOR surfactant on sand grains was firstly studied in DI water and in brine. Next, static adsorption of PEC was investigated, followed by the discussion of the influencing factors.

4.2.1.1.1 Static adsorption of sulfate surfactant

The starting solution concentration of sulfate surfactant was 1%. To study the adsorption of surfactant in DI water, the surfactant solution was diluted to 0.5% using DI water; for

the surfactant adsorption study in brine, the surfactant solution was diluted to 0.25% using brine. Berea sandstone and carbonate sand were crushed and sieved through 100 and 50 mesh screen to obtain sand grains with diameter between 150 and 300 um. 15g diluted sulfate surfactant solution was agitated with 1.5g sand grains at room temperature at 160 rpm of shaking speed for different shaking time periods. After agitation, the supernatant was taken out, centrifuged at 4,000 rpm for 10 minutes, and filtered through 0.2 um syringe filter to remove as much suspended solids as possible. Then, TOC method was used to analyze the concentration of surfactant in the solution before and after agitation.

4.2.1.1.2 Static adsorption of PEC

To investigate the adsorption mechanism of PEC, 1.5g sandstone grains was stirred with 15g prepared PEC suspension at room temperature at 220 rpm of shaking speed for different time periods. After agitation, the supernatant was taken out and filtered through 0.45 um syringe filter. The agitated and filtered PEC supernatant solution was analyzed using TOC/TN analytical method.

4.2.1.1.3 Factors influencing static adsorption of PEC

Two factors influencing static adsorption were investigated, electrolyte concentration and sand type. The prepared PEC suspension was diluted using DI water and brine at 1:1 of weight ratio, respectively. 1.5g sand grains (Berea sandstone or carbonate) were stirred with 15g diluted PEC suspension at 160 rpm of shaking speed at room temperature. The supernatant was taken out and filtered through 0.45 um syringe filter after different time

periods of shaking. Agitated and filtered PEC supernatant solution was analyzed using TOC/TN analytical method to discuss the influencing factors.

4.2.1.2 Analytical method

4.2.1.2.1 TOC method for surfactant concentration measurement

Total organic carbon and nitrogen concentrations in sulfate surfactant and PEI solutions were firstly estimated to determine the range of TC, IC, and TN calibration curves. Through analyzing the chemical formula of sulfate surfactant and PEI and the optimized PEC preparation protocol, the appropriate ranges of TC, IC, and TN calibration curves are 100 to 800 ppm, 100 to 500 ppm, and 2 to 20 ppm, respectively.

To create TC calibration curve, 1,000 ppm TC standard solution was used as stock solution and diluted to 100 ppm, 200 ppm, 400 ppm, 600 ppm, and 800 ppm. Meanwhile, several instrument parameters (injection volume and integration time) were optimized to avoid oversaturating the detector and obtain a better linearity of calibration curve. Calibration curves are valid for one week. Fig. 15 showed an example of TC calibration curve obtained directly from TOC-L instrument.

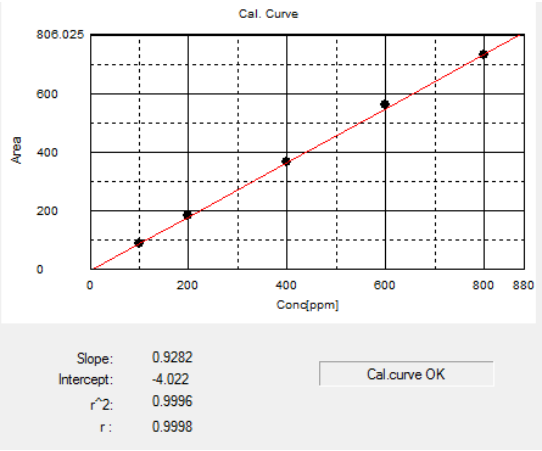

Figure 15 TC calibration curve ranging from 100 to 800 ppm

Similar procedures were followed to obtain IC and TN calibration curves (See Fig. 16 and Fig. 17).

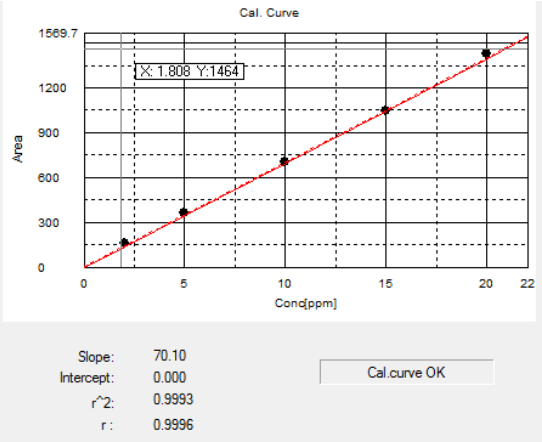

Figure 16 IC calibration curve ranging from 2 to 20 ppm

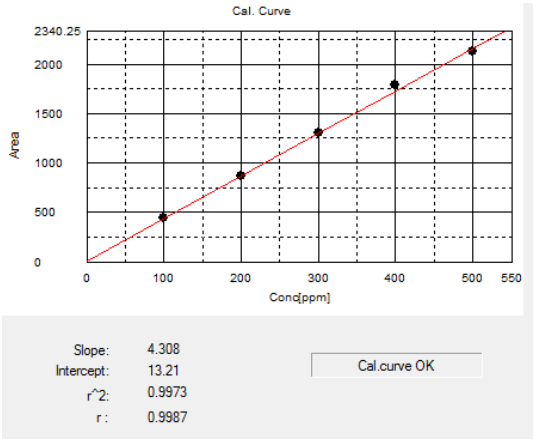

Figure 17 TN calibration curve ranging from 100 to 500 ppm

The relationship between sulfate surfactant and TOC concentration was obtained (Fig.18) using these calibration curves with good linearity. The concentration of sulfate surfactant before and after static adsorption test was calculated from TOC concentration using the linear fitting formula shown in Fig.18.

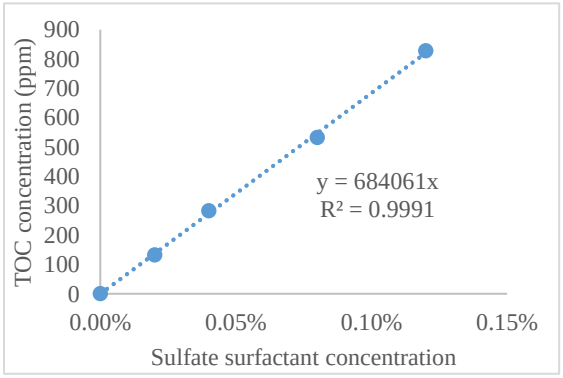

Figure 18 Relationship between sulfate surfactant and TOC concentration

4.2.1.2.2 TOC/TN method for PEC analysis

PEC suspension inevitably contains surfactant entrapped in PEC, free surfactant and free PEI. In order to better analyze the composition in PEC suspension, an effective TOC/TN method is required.

(a)

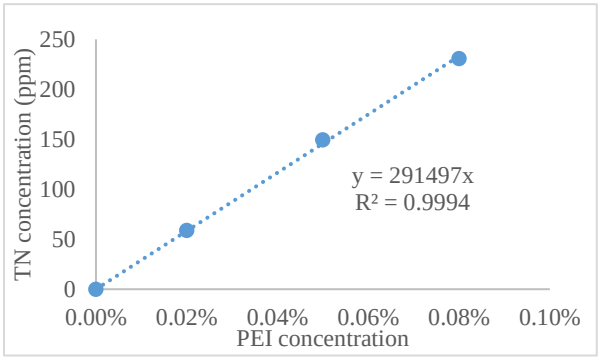

(b)

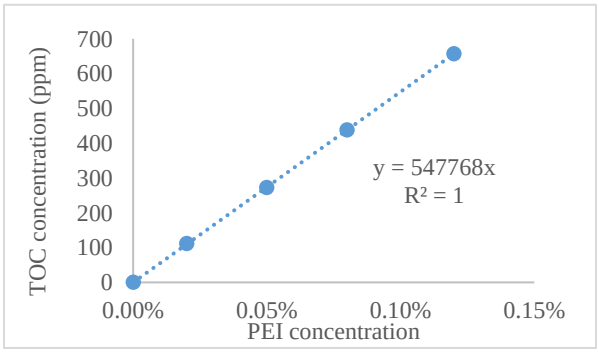

Figure 19 Relationship between (a) PEI and TN concentration and (b) PEI and TOC concentration

Firstly, the correlations between PEI and TOC concentration, PEI and TN concentration were built up (See Fig. 19). In PEC suspension, PEI is the only chemical containing nitrogen element while there are two sources of TOC, surfactant and PEI. In terms of the

mathematics matrix thoughts, the relationship between TOC/TN and surfactant/PEI is expressed as follows.

$$\begin{bmatrix} a & 0 \\ b & c \end{bmatrix} \begin{bmatrix} TOC \\ TN \end{bmatrix} = \begin{bmatrix} [surfactant] \\ [PEI] \end{bmatrix}$$

Where a represents surfactant/TOC calibration cure, b represents PEI/TOC calibration curve, c represents PEI/TN calibration curve.

Therefore, TOC/TN method for PEC analysis is designed as follows (Fig. 20): firstly, TOC and TN concentrations of PEC suspension are measured, referred to as TOC_{total} andTN_{total}; secondly, the concentration of PEI (include both free PEI and PEI from surfactant entrapped in PEC) can be calculated by TN_{total} using the fitting formula in Fig. 19 (a); thirdly, TOC concentration from PEI (TOC_{PEI}) is calculated with the calculated PEI concentration using the fitting formula in Fig.19 (b); TOC concentration from surfactant ($TOC_{surfactant}$) can be then obtained by subtracting TOC_{PEI} from TOC_{total}, expressed as $TOC_{surfactant} = TOC_{total} - TOC_{PEI}$; finally, with the calculated $TOC_{surfactant}$, the concentration of surfactant is obtained using the fitting formula in Fig.18.

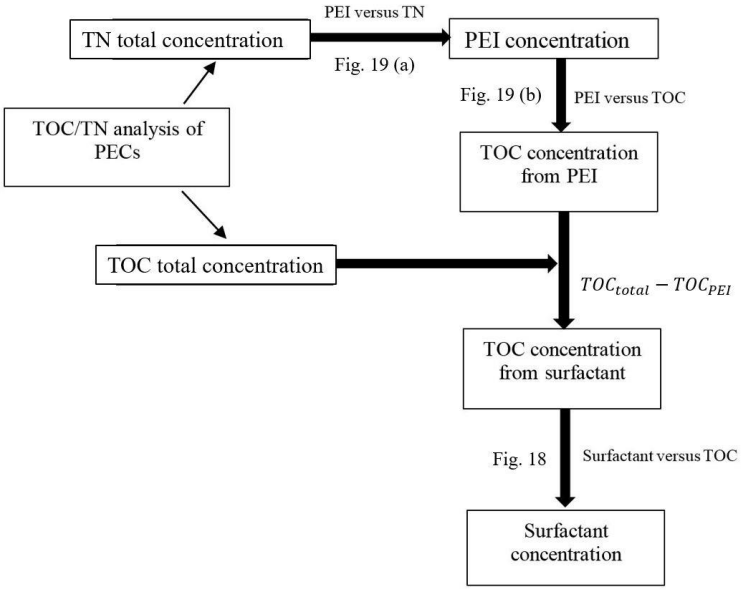

Figure 20 TOC/TN method for PEC analysis

In addition, PEC exists in solution as colloidal system and static adsorption will be run in brine. Therefore, the validation of TOC/TN analytical method for PEC analysis in DI water and in brine requires to be tested to make sure there is no interference from the colloidal system and electrolyte. Synthetic brine was prepared based on Table 1.

Table 1 Recipe of synthetic brine

Composition	NaCl	KCl	$CaCl_2$-$2H_2O$	$MgCl_2$-$6H_2O$	Na_2SO_4	DI water
Weight (g)	26.22	0.166	0.444	1.414	0.37	969.2

In DI water adsorption test, PEC suspension was diluted 10 times to make it within the range of calibration curves. In brine adsorption test, PEC suspension was mixed with synthetic brine using 1:1 of weight ratio, followed by 10 times of dilution. The measured

values obtained using TOC/TN method were compared to the theoretical values to confirm the validation of TOC/TN method for PEC analysis.

4.2.2 Real-time adsorption study by QCM-D

4.2.2.1 Real-time adsorption of surfactant

Real-time adsorption of sulfate surfactant was analyzed using QCM-D instrument and negatively charged silicon sensor. The silicon sensor was firstly treated by UV/O_3 for ten minutes then immersed in 2% SDS solution for 30 minutes at room temperature. The sensor was then rinsed with DI water, dried with nitrogen gas and treated by UV/O_3 for another ten minutes. Finally the sensor could be placed in the module and ready for the measurement.

The procedure of real-time adsorption of sulfate surfactant was as follows: firstly, sensor was flushed by DI water at fixed speed of 150 ul/min to set up a baseline; 0.5% of sulfate surfactant solution was then pumped to the silicon sensor until frequency and dissipation reached an equilibrium, followed by incubation process; lastly, silicon sensor was rinsed with DI water to flush away the loosely adsorbed materials. After the measurement, the module and sensor were cleaned by 2% of SDS solution, DI water and dried using nitrogen gas.

4.2.2.2 Real-time adsorption of PEC: confirmation of PEC adsorption model

Same sensor cleaning protocols were conducted before measurement. The procedure of PEC real-time adsorption was designed as follows. Firstly, experiment started with DI water to build up a baseline (step 1). Secondly, the prepared PEC suspension was diluted

50 times and kept injecting to the sensor until frequency and dissipation reached an equilibrium (step 2). A subsequent incubation with PEC suspension was followed to stabilize the adsorbed PEC on surface and to monitor the change of adsorbed mass (step 3). Sensor was then rinsed with DI water until frequency and dissipation reached an equilibrium again (step 4). Next, 0.5% of sulfate surfactant solution was injected to the sensor (step 5). Another incubation with surfactant solution was followed (step 6). The rinsing schedule for PEC real-time adsorption is shown in Table 2.

Table 2 Rinsing schedule for PEC real-time adsorption

Material	DI water	PEC suspension	Incubation with PEC suspension	DI water	Surfactant solution	Incubation with surfactant solution
Step	1	2	3	4	5	6

CHAPTER V

RESULTS AND DISCUSSION

5.1 Bulk properties of PEC

5.1.1 Characterization of PEC

5.1.1.1 Optimization of PEC

5.1.1.1.1 Effect of surfactant/PEI stock solution concentrations

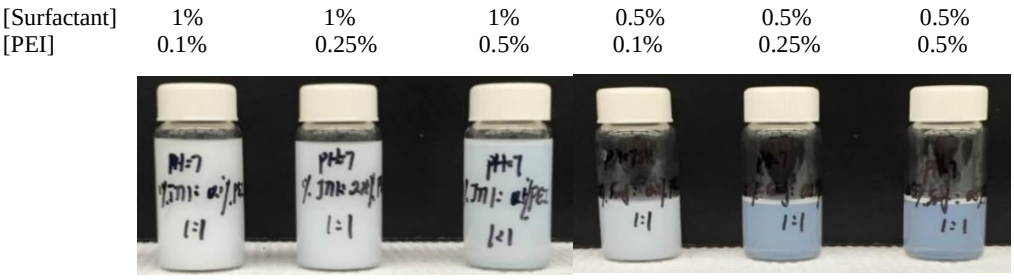

Figure 21 PEC suspensions of different surfactant/PEI concentrations at fixed surfactant to PEI (pH 7) weight ratio of 1:1

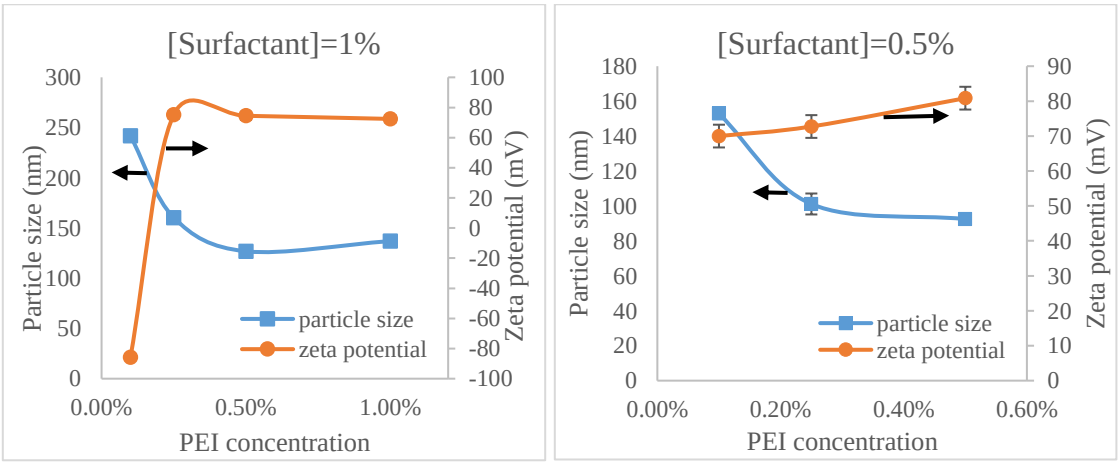

Figure 22 Particle size and zeta potential of PEC as a function of surfactant/PEI concentrations at fixed surfactant to PEI (pH 7) weight ratio of 1:1

The effect of surfactant/PEI stock solution concentrations on the characteristics of PEC was firstly discussed. 1% and 0.5% of sulfate surfactant solutions were mixed with 0.5%, 0.25%, and 0.1% of PEI solutions (pH 7) respectively at fixed surfactant to PEI weight ratio of 1:1 (Fig. 21 shows the appearance of PEC suspensions). Measurement of particle size and zeta potential (shown in Fig.22) revealed that with the increase of PEI concentration particle size decreased and then reached a plateau. On the other hand, zeta potential was around +80mV, independent of surfactant and PEI concentrations. But when 1% of sulfate surfactant solution was mixed with 0.1% of PEI solution (pH 7) at weight ratio of 1:1, negatively charged PEC with zeta potential of -85mV was obtained. This may be explained by the positive charges on PEI compensated by large amounts of negative charges from anionic surfactant with high surfactant concentration.

5.1.1.1.2 Effect of surfactant to PEI weight ratio

(a)

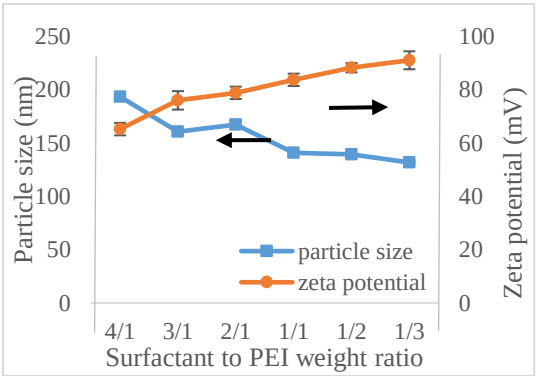

Figure 23 (a) Particle size and zeta potential of PEC as a function of surfactant to PEI weight ratio and (b) PEC suspensions of different surfactant to PEI weight ratios at fixed surfactant/PEI (pH 7) concentrations of 1%

(b)

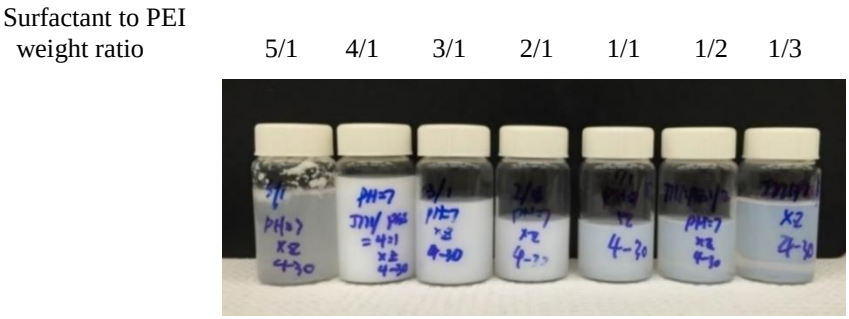

Figure 23 Continued

The effect of surfactant to PEI weight ratio on PEC properties was discussed at fixed surfactant/PEI (pH 7) concentrations of 1%. Fig. 23 (a) showed that zeta potential decreased and particle size increased with the increasing surfactant to PEI weight ratio. That is because with the increasing surfactant to PEI weight ratio, more surfactant is present in the system thus more positive charges of PEI will be neutralized by the negative charges from the surfactant. Based on the DLVO theory (Ghosh), the reduction of zeta potential leads to the lower energy barrier which makes the charged colloidal system easier to coagulate and further increases particle size. Furthermore, the appearance observation (Fig. 23 (b)) showed that PEC started to aggregate at surfactant to PEI weight ratio of 5:1. It is known that the net charge and the barrier energy provides long-term stability to the colloidal system by inhibiting aggregation (Gao et al. 2013). The surfactant to PEI weight ratio of 5:1 reduced the net charge to a value below which the repulsion force can no longer stabilize the PEC colloidal system.

5.1.1.1.3 Effect of PEI pH

(a)

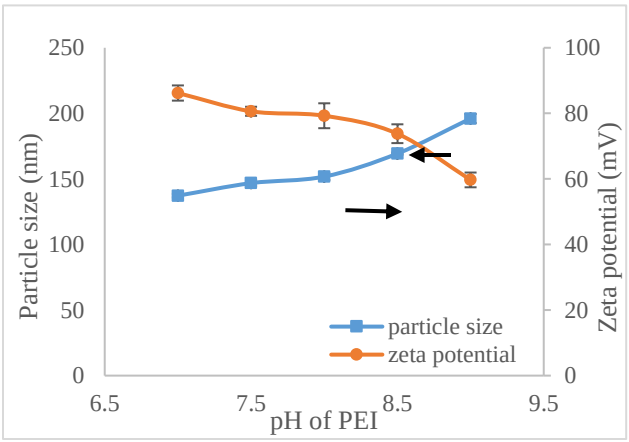

(b)

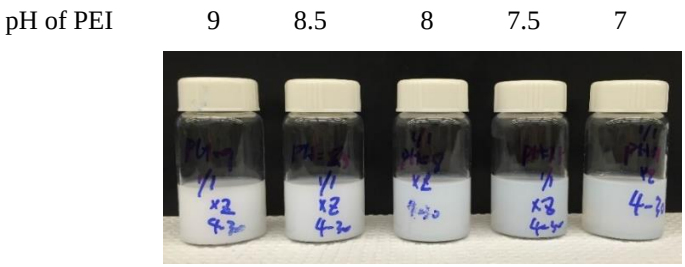

Figure 24 (a) Particle size and zeta potential of PEC as a function of PEI pH and (b) PEC suspensions of different PEI pH at fixed surfactant/PEI concentrations of 1% and surfactant to PEI weight ratio of 1:1

pH of PEI solution has a significant effect on the characteristics of PEC because PEI is a weak polyelectrolyte and the charge of PEI is determined by pH environment. The effect of PEI pH was investigated by changing the pH of PEI solution from 9.0 to 7.0 at fixed 1% of surfactant/PEI concentrations and 1:1 of weight ratio. Measurement of particle size and zeta potential (Fig. 24 (a)) showed that particle size decreased and zeta potential increased with the decrease of PEI pH. When pH of PEI decreases, the positive charge density on

PEI increases thus zeta potential of PEC increases. Higher zeta potential leads to larger energy barrier and the repulsion force between PECs which reduces the tendency of charged particles to coagulate and decreases particle size (Ghosh).

5.1.1.2 Stability test of PEC

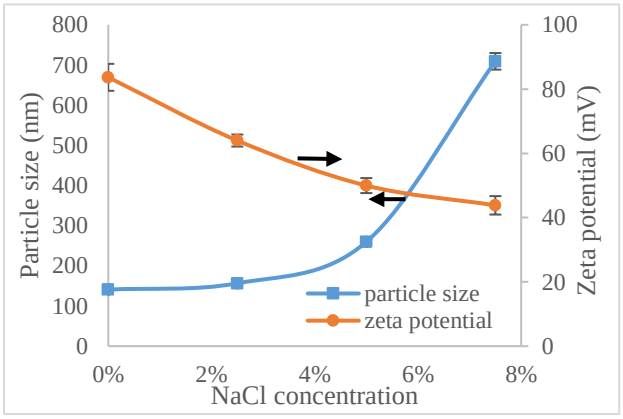

Figure 25 Particle size and zeta potential of PEC at different NaCl concentrations

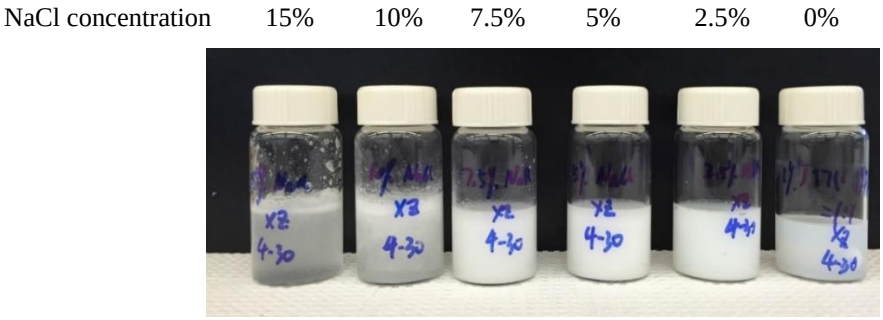

Figure 26 PEC suspensions at different NaCl concentrations

The stability of PEC was investigated in different concentrations of NaCl solutions. Sodium chloride powders were added into PEC suspension to make different sodium chloride concentrations (2.5%, 5%, 7.5%, 10%, and 15%) in PEC suspension. With the

increasing NaCl concentration, zeta potential kept decreasing whereas particle size remained unchanged up to 2.5% of NaCl solution, beyond which a sharp increase was observed (shown in Fig. 25). Appearance observation (Fig.26) showed that PECs started to aggregate when NaCl concentration reached 7.5%. Furthermore, significant precipitation appeared when NaCl solution reached 15%. This observation agreed well with the result of Gao (2014) and the DLVO theory, where the increasing ionic strength coagulates the particles by decreasing the length of double layer (Yu et al. 2010) and the energy barrier (Ghosh) avoiding coagulation. Solomatin et al. (2003) also proposed that the addition of electrolyte solution partially screens out electrostatic interaction, reduces zeta potential and aggregates particles.

5.1.1.3 PEC surfactant EE measurement

5.1.1.3.1 Methylene blue UV spectroscopy method for PEC surfactant EE measurement

PEC suspension after four times of centrifugation

PEC suspension after one time of centrifugation

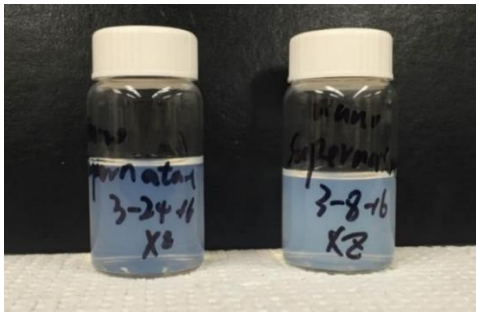

Figure 27 Supernatants of PEC suspensions after (a) one time of centrifugation and (b) four times of centrifugation

Table 3 PEC surfactant EE results using MB UV spectroscopy method

(1^{st} and 2^{nd} measurement refer to the same sample measured twice)

	Dilution times	EE
1^{st} measurement	195	58.87%
	352	44.74%
2^{nd} measurement	295	43.07%
	504	21.08%

Surfactant EE of the prepared PEC was measured with different dilution times using UV spectroscopy method (results of two times of measurement are shown in Table 3). If the method was valid for PEC surfactant EE measurement, results from different dilution times and different measurement were supposed to be similar. However, the results listed in Table 3 showed that measured EE values of different dilution times and different measurement did not agree with each other. This problem may due to the interferences from PECs to UV absorbance. We noticed that the appearance of supernatants after four times of centrifugation were still translucent (Fig.27), which suggested the existence of a large amount of suspended PECs. The existence of the suspended PECs in the supernatant was the main factor interfering UV absorbance measurement of surfactant-MB pair and made the measured EE values random and unreliable.

5.1.1.3.2 Methylene blue titration method for PEC surfactant EE measurement

In MB titration method, anionic surfactant is extracted quantitatively by cationic hyamine from aqueous phase to organic phase, and the titration ending point is determined through observing the variation of solution color. Started with the surfactant test using MB titration method (See Table 4). The small error between theoretical and measured values proved the validation of MB titration method to measure surfactant concentration.

Table 4 Surfactant test of MB titration method

Surfactant theoretical concentration	Measured surfactant concentration	Error
0.1499 %	0.154 %	2.70 %
0.2004 %	0.210 %	4.79 %
0.2864 %	0.301 %	5.10 %

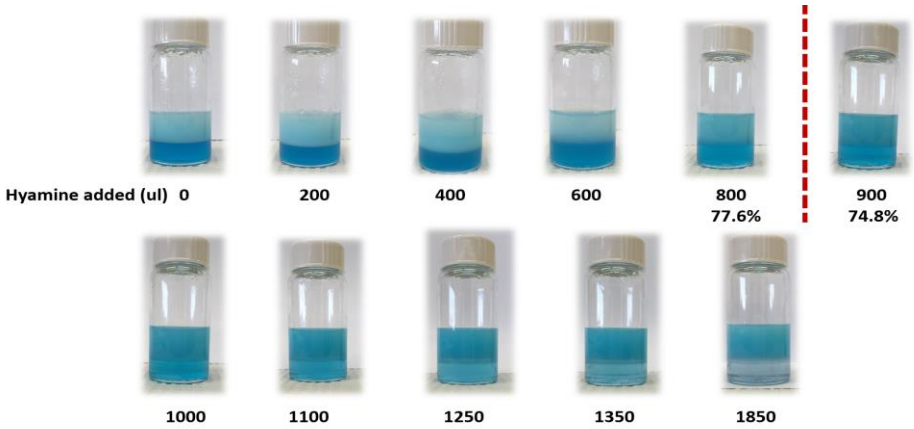

Figure 28 One case of surfactant EE measurement using MB titration method

One case example of surfactant EE measurement of the prepared PEC using MB titration method is illustrated in Fig. 28. The supernatant of prepared PEC suspension was mixed with DI water, stabilized MB and chloroform as is discussed in Chapter 4. Before titration, two layers will appear in this mixture. The upper aqueous layers looked colorless and lower organic layers, which dissolved MB-surfactant pair, looked blue. The change of color was observed and recorded after each small addition of hyamine into the solution (Fig.28). In this case measurement, when 800ul of hyamine was added to the solution, the upper aqueous layer looked a little lighter than lower organic layer. But after another 100ul of hyamine was added, the upper aqueous layer turned darker than lower organic layer. So

the ending point of MB titration method was considered as 900ul of hyamine, which was transformed to 75% of EE calculated using equation (1) and (2). Based on several times of measurements, surfactant EE of prepared PEC was calculated as 77.1 ± 2.1 % using MB titration method.

5.1.2 Surfactant release from PEC test

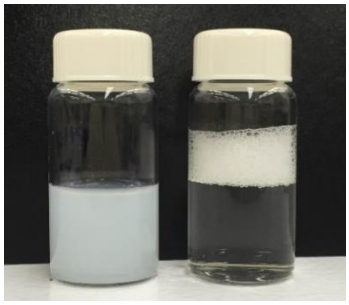

Figure 29 Unreleased PEC suspension (left) and released PEC suspension after the addition of Na2CO3 (right)

During the EOR process, surfactant is the functional chemical that reduces IFT between oil and water and changes the wettability of rock surface. Therefore, surfactants need to be released to take effect after long-time delivery by PEC in porous rock media. Certain amounts of Na_2CO_3 solid powders were added into PEC suspension to make 1% Na_2CO_3 in PEC suspension. Fig. 29 revealed that the milky colloidal system became clear and transparent right after the addition of sodium carbonate powders. MB titration method was then utilized to measure the surfactant concentration in released PEC suspensions.

Table 5 Surfactant release from PEC test using MB titration method

Measured surfactant concentration	Theoretical surfactant concentration
0.518%	0.5%

Since PEC was prepared through mixing 1% of sulfate surfactant and PEI solutions at weight ratio of 1:1, in PEC suspension the theoretical value of total surfactant concentration (including free surfactant and surfactant entrapped by PEI) is 0.5%. The measured surfactant concentration in PEC suspension after the addition of sodium carbonate was 0.518% (Table 5), which agreed well with theoretical value. This agreement indicated that after the addition of sodium carbonate all surfactants were able to be detected by MB titration method. Since MB titration method only measures the concentration of free surfactant in solution, all surfactants entrapped in PEC were thus released after the addition of sodium carbonate.

5.2 Adsorption study of PEC

5.2.1 Static adsorption study

5.2.1.1 Validation of TOC/TN analytical method for PEC analysis

Table 6 Validation test of TOC/TN analytical method for PEC analysis

Environment	Measured value		Theoretical value	
	Surfactant (%)	PEI (%)	Surfactant (%)	PEI (%)
DI water	0.047%	0.051%	0.05%	0.05%
Brine	0.024%	0.025%	0.025%	0.025%

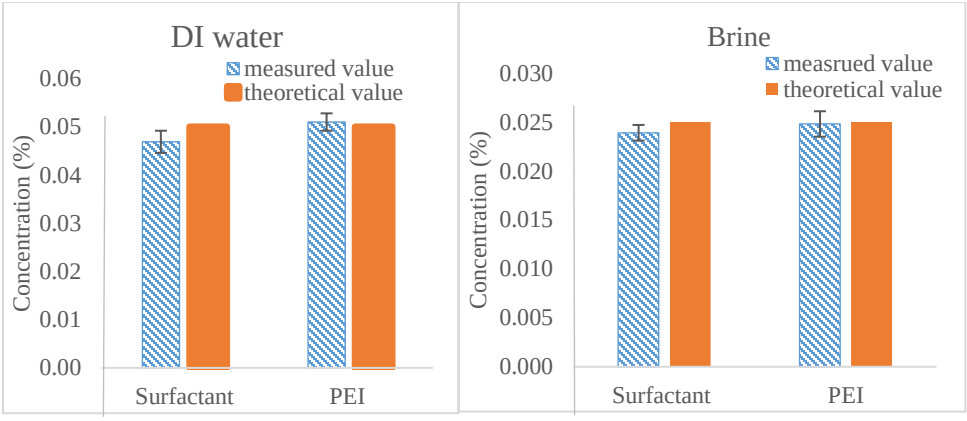

Figure 30 Validation test of TOC/TN analytical method for PEC analysis

The validation tests of TOC/TN analytical method for PEC analysis in DI water and in brine were performed to make sure that the colloidal system and electrolyte do not introduce interference to measurement. For PEC prepared in DI water, the theoretical concentrations of surfactant and PEI are both 0.5%. After PEC suspension was diluted 10 times, the measured surfactant and PEI concentrations were 0.047% and 0.051%, respectively. The prepared PEC suspension was mixed with brine at 1:1 of weight ratio and the theoretical concentrations of surfactant and PEI are both 0.25%. After PEC suspension prepared in brine was diluted 10 times the measured surfactant and PEI concentrations were 0.024% and 0.025%, respectively (results shown in Table 6 and Fig.30). The errors between measured and theoretical values were less than 10% for PEC suspension prepared in both DI water and brine. Therefore, TOC/TN analytical method discussed in Chapter 4 proved to be valid for PEC analysis in the existence of electrolyte and colloidal particles.

5.2.1.2 Static adsorption of surfactant

(a)

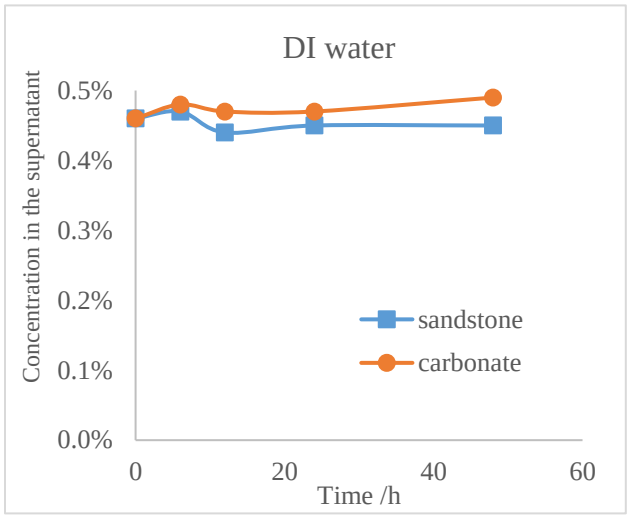

(b)

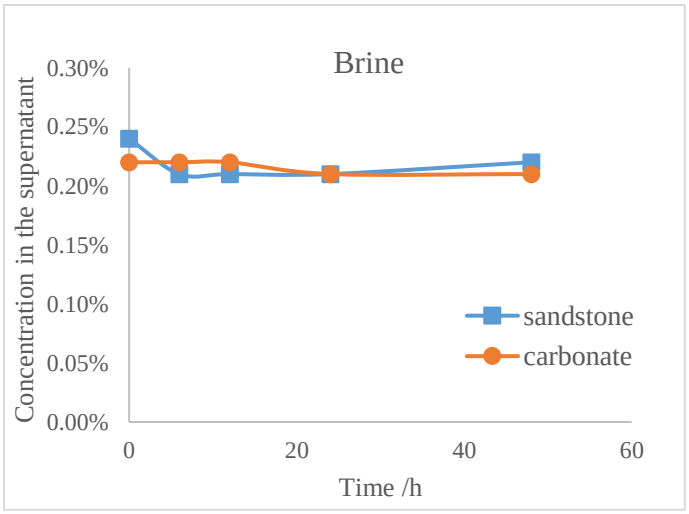

Figure 31 Concentration of sulfate surfactant in the supernatant varies with time during surfactant adsorption on sand grains (a) in DI water and (b) in brine

Static adsorption of sulfate surfactant was performed in both DI water and brine. As adsorption proceeded, TOC concentration of surfactant supernatant solution was

measured, transformed to sulfate surfactant concentration and plotted with different times (6h, 12h, 24h and 48h) (Fig. 31). For adsorption in DI water, the initial surfactant concentration was 0.5%. After 2 days of shaking, the concentration remained the same. Similar results were observed for surfactant adsorption in brine. NanoBrook Omni was used to measure the surface charge of sand grains. The surface charges of sandstone and carbonate sand grains in DI water are -70mV and -25 mV, respectively; and in brine the surface charges of sandstone and carbonate sand grains became -20mV and -8 mV, respectively. Since sulfate surfactant is anionic, there exists large electrostatic repulsion between the anionic surfactant and the negatively charged sand. Therefore, sulfate surfactant does not have a tendency to be adsorbed by the negatively charged sand grains in both DI water and brine.

5.2.1.3 Static adsorption of PEC

Adsorption percentage, expressed as the following equation, was used to study the static adsorption of PEC.

$$\text{AD}\ (\%) = \frac{C_{initial} - C_{after}}{C_{initial}} \times 100\% \quad (3)$$

Where AD represents adsorption percentage, $C_{initial}$ represents initial concentration of surfactant or PEI in PEC suspension before adsorption test, and C_{after} is the concentration of surfactant or PEI in PEC suspension after adsorption test.

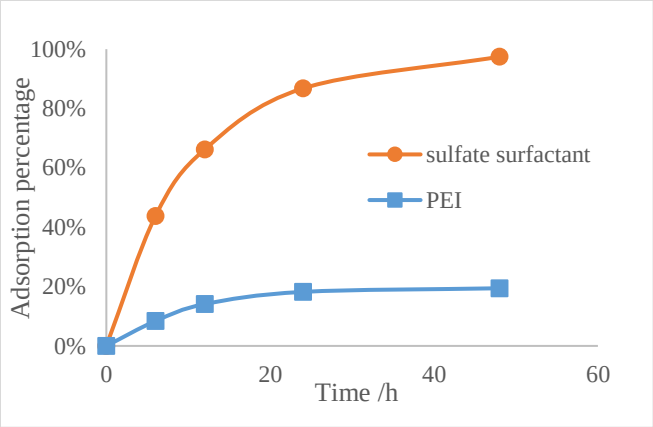

Figure 32 Adsorption percentage of surfactant and PEI in PEC suspension on sandstone in DI water

The adsorption percentage of PEC on sandstone in DI water was obtained (Fig.32) using TOC/TN analytical method and equation (3). In Fig.32, the adsorption percentage of both surfactant and PEI in PEC suspension showed a similar trend. At the beginning, the adsorption rate increased rapidly; with the time passing by, the increase of adsorption rate slowed down and reached a maximum value. The rapid adsorption rate observed at the beginning is probably due to the abundant availability of active sites on the surface of sand grains, and with the gradual occupancy of these sites by particles, the adsorption process slows down. When adsorption time lasts long enough, the active sites on the surface of sand grains are fully occupied by adsorbates (Baskaralingam et al. 2006). Thus the adsorption process reached equilibrium where the adsorption percentage became unchanged.

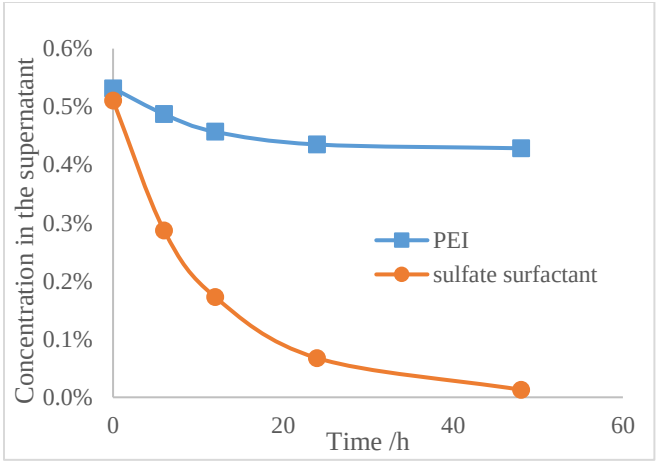

Figure 33 Supernatant concentrations of surfactant and PEI in PEC suspension versus time during PEC adsorption on sandstone in DI water

Fig.33 shows the change of surfactant and PEI concentrations in PEC supernatant solution as a function of adsorption time. After adsorption reached equilibrium, a larger decrease of surfactant concentration than PEI concentration in PEC supernatant solution was observed. PEI concentration decreased from 0.54% to 0.42%, whereas surfactant concentration decreased from 0.51% to below 0.02%. This result revealed that there was little surfactant left in the supernatant after 48 hours of shaking.

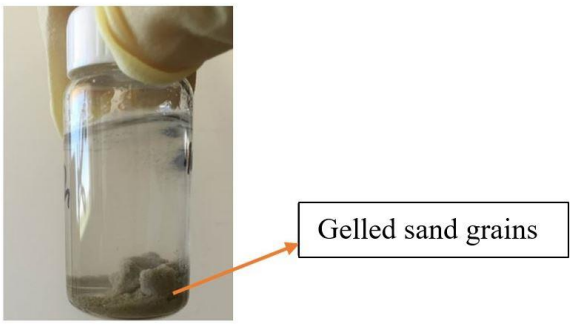

Figure 34 PEC suspension after 48 hours of shaking with sandstone sand grains

Shaking time 6 h 12 h 24 h 48 h

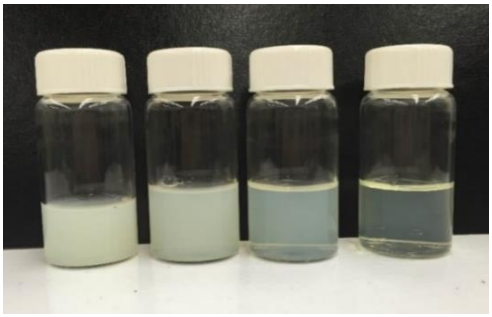

Figure 35 PEC supernatants after shaking with sandstone sand grains for different time periods in DI water

In addition to quantitative analysis, similar results were obtained from the appearance observation of PEC suspensions after shaking with sandstone grains. Fig. 34 showed that sand grains were gelled to a ball shape after shaking for two days with PEC suspension, which may result from the high shaking speed and the adsorbed PEC particles. In addition, longer shaking time led to less milky and clearer PEC supernatant solution (see Fig. 35), which corresponded to less PECs left in the supernatant. The PEC supernatant after 48 hours of shaking with sandstone grains was taken for particle size measurement. NanoBrook Omni read a count rate of 13 kcps, whereas less than 50 kcps of count rate indicates that no or very low concentration of nanoparticles are present in the solution. Thus, based on above observations, almost all PECs were adsorbed after two days of agitation with sandstones in DI water.

In order to investigate the variation of sand surface property after shaking with PEC suspension, the following experiment was carried out. After PEC suspension was agitated with sandstone grains for two days, the supernatant was aspirated from the vial. 15 g of

0.5% sulfate surfactant solution was then added into the vial and agitated with the PEC treated sandstone grains for another 24 hrs. After 24 hours of shaking, the supernatant was filtered through 0.2 um syringe filter and TOC method was then followed to analyze the change of sulfate surfactant concentration in the supernatant.

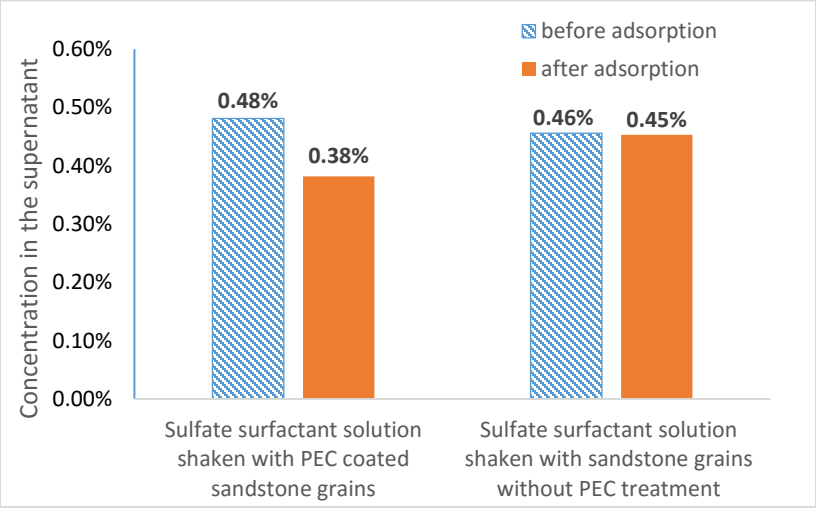

Figure 36 Sulfate surfactant concentrations before and after adsorption on PEC coated sandstone grains and sandstone grains without PEC treatment

The TOC results showed 20% decrease of sulfate surfactant concentration after 0.5% of sulfate surfactant solution was agitated with PEC treated sandstone grains for 24 hours (Fig.36). Whereas the adsorption of sulfate surfactant on sandstone grains without PEC treatment is almost zero (Fig.31). It can be inferred that the sandstone grains agitated with PEC are more likely to adsorb surfactant compared to those without PEC treatment. Based on these observations, a hypothesis of PEC adsorption model was proposed. When positively charged PEC suspension (including free PEI, free surfactant and PEC) is shaken with negatively charged sand grains, a large amount of PEC nanoparticles (+) and a small

amount of PEI (+) will firstly be adsorbed on the surface of sand grains (-) to form the first layer. Moreover, nanoparticle will distort on the surface to have a larger surface area. After the formation of PEC/PEI layer (+), free anionic surfactants will be adsorbed onto the PEC/PEI coated sand surface due to electrostatic attraction and the increasing surface area of the distorted PEC nanoparticles (Fig. 37). Based on this proposed model, the wettability of a negatively charged rock surface may be changed by an anionic surfactant entrapped in PEC because the hydrophilic head of surfactant adsorbed onto PEC/PEI coated surface can make surface more water-wet.

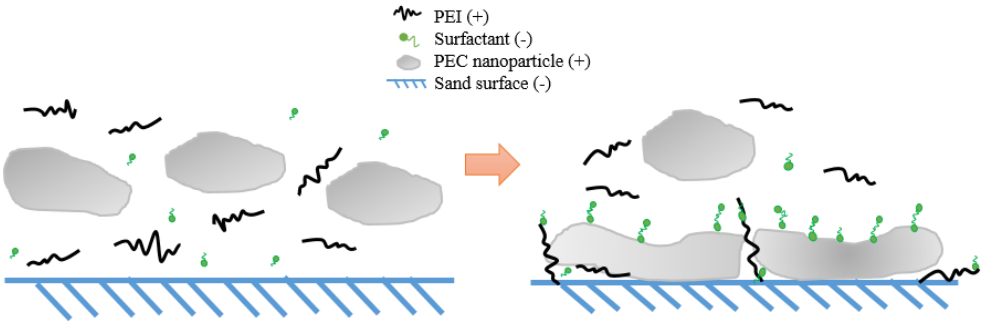

Figure 37 Schematic of PEC adsorption model

5.2.1.4 Factors influencing PEC adsorption

5.2.1.4.1 Salinity effect

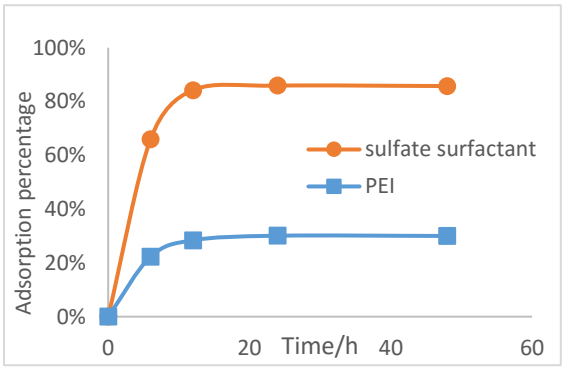

Figure 38 Adsorption percentage of surfactant and PEI in PEC suspension on sandstone in brine

To study the effect of salinity on PEC adsorption, PEC suspension was agitated with sand grains in DI water and in brine. Adsorption percentage of PEC on Berea sandstone in brine was illustrated in Fig.38. At the beginning, the adsorption rate increased rapidly and then slowed down to a plateau where no more adsorbates could be adsorbed onto sandstone surface.

(a) Brine

Shaking time 0 h 6 h 12 h 24 h 48 h

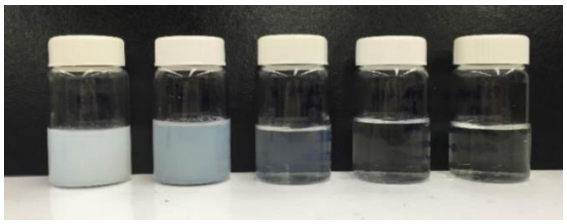

(b) DI water

Shaking time 0 h 6 h 12 h 24 h 48 h 84 h

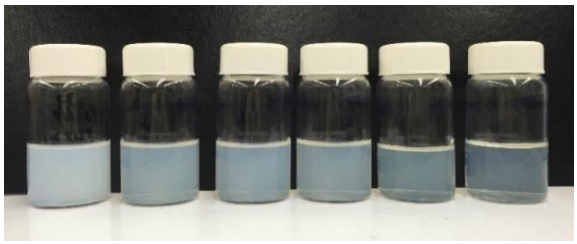

Figure 39 Supernatants of PEC suspensions after shaking with sandstone sand grains for different time periods (a) in brine and (b) in DI water

(a) Brine

Shaking time 0 h 6 h 12 h 24 h 48 h

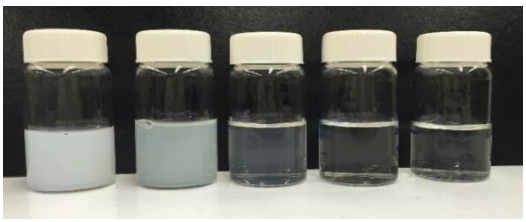

(b) DI water

Shaking time 0 h 6 h 12 h 24 h 48 h 84 h

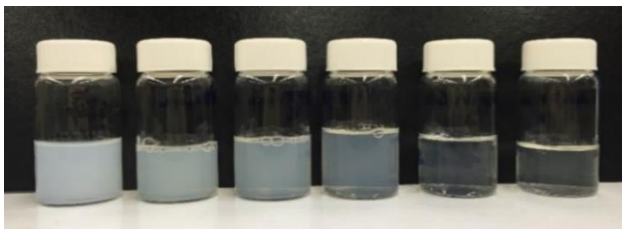

Figure 40 Supernatants of PEC suspensions after shaking with carbonate sand grains for different time periods (a) in brine and (b) in DI water

The appearance observation (shown in Fig.39 and Fig.40) illustrated that it took less time for PEC suspension to become clear during the adsorption test in brine than in DI water. In brine, PEC suspension looked almost clear after 12 hrs of agitation, whereas in DI water it looked little milky after 84 hrs. The clearer the solution looked, the less PEC nanoparticles were present in solution.

(a)

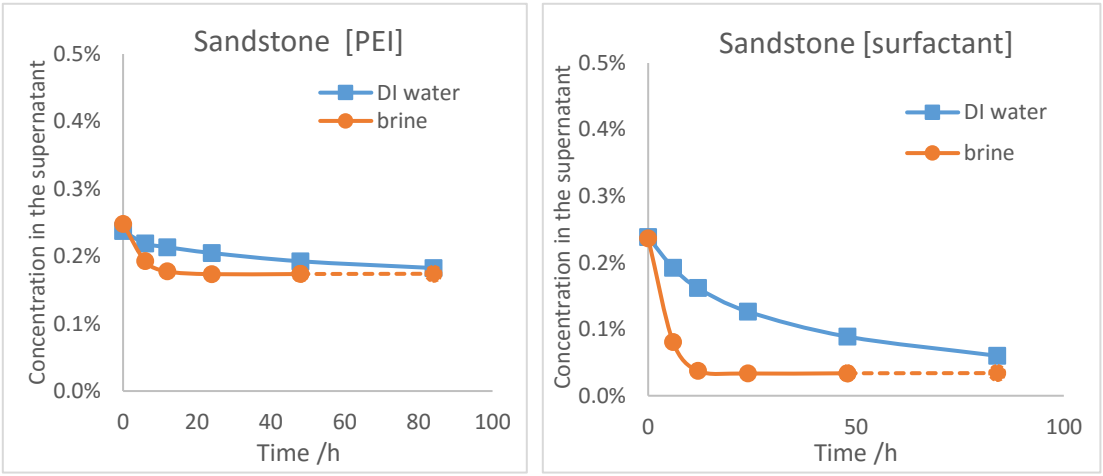

(b)

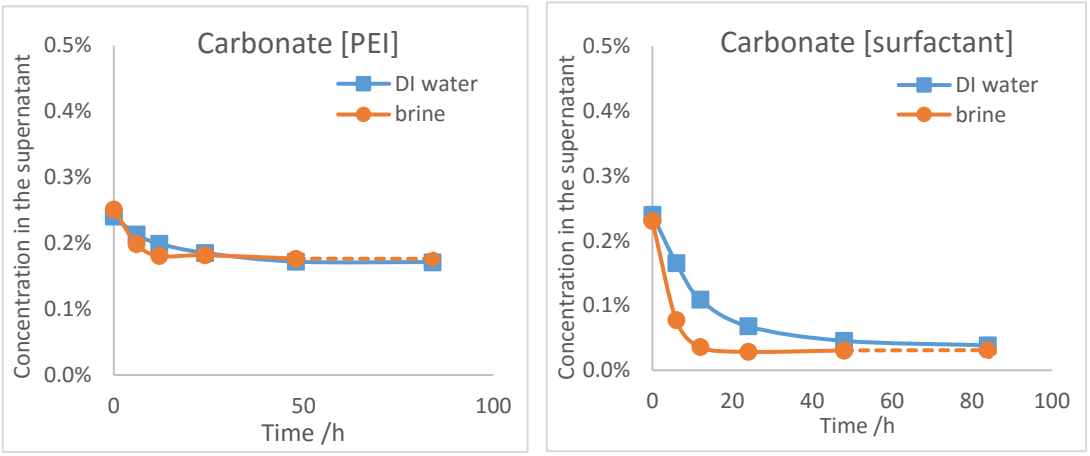

Figure 41 Comparison of surfactant and PEI adsorption in PEC suspension on (a) sandstone and (b) carbonate sand in DI water and brine

Moreover, TOC/TN analytical method was used to analyze the concentration change of surfactant and PEI in PEC supernatant during adsorption test in DI water and in brine (results shown in Fig. 41). It was observed that for PEC adsorption in brine, the supernatant concentrations of both PEI and surfactant reached an equilibrium after 12 hrs of shaking; on the contrary, for PEC adsorption in DI water, the time to reach an equilibrium was 84 hours or even longer. Another observation was that the equilibrium concentrations of surfactant and PEI for PEC adsorption in DI water were similar to PEC adsorption in brine. For example, in terms of PEC adsorption on carbonate, the supernatant concentrations of PEI and surfactant decreased from 0.25% to 0.17% and 0.03%, respectively, in both DI water and brine (Fig. 41). It seems that the existence of electrolyte in solution speeds up the adsorption of PEC but not increases the eventual adsorbed mass. The observation that increasing ionic strength accelerates the adsorption of PEC can be explained by the DLVO theory. The double layer of PEC particles tends to shrink at high ionic strength solution, then zeta potential and energy barrier decreases significantly, which further reduces the repulsion force between adsorbed charged PEC and accelerates adsorption (Yu et al. 2010). However, the availability of active sites on surface is same in DI water and in brine. When all active sites on the surface are fully occupied by materials, surface is saturated and can no longer adsorb anything. Therefore, the existence of electrolyte in solution accelerates the adsorption of PEC not increases the eventual adsorbed mass.

5.2.1.4.2 Sand type effect

(a)

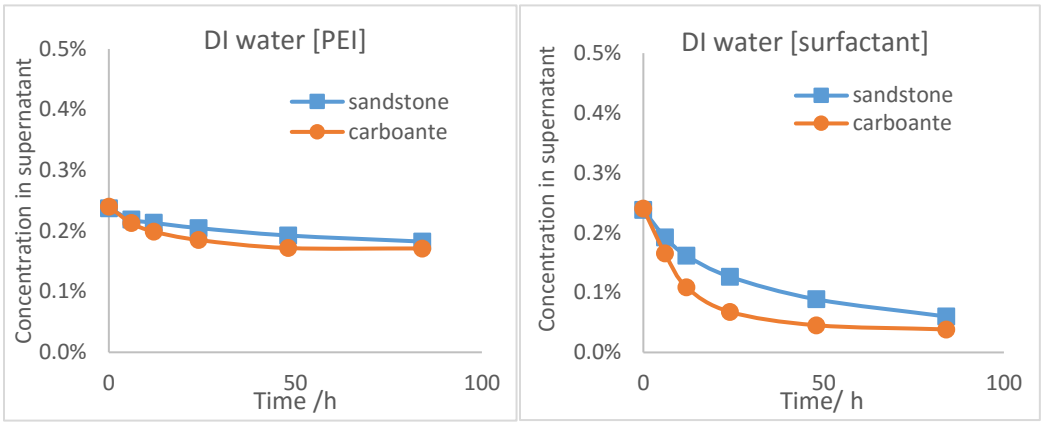

(b)

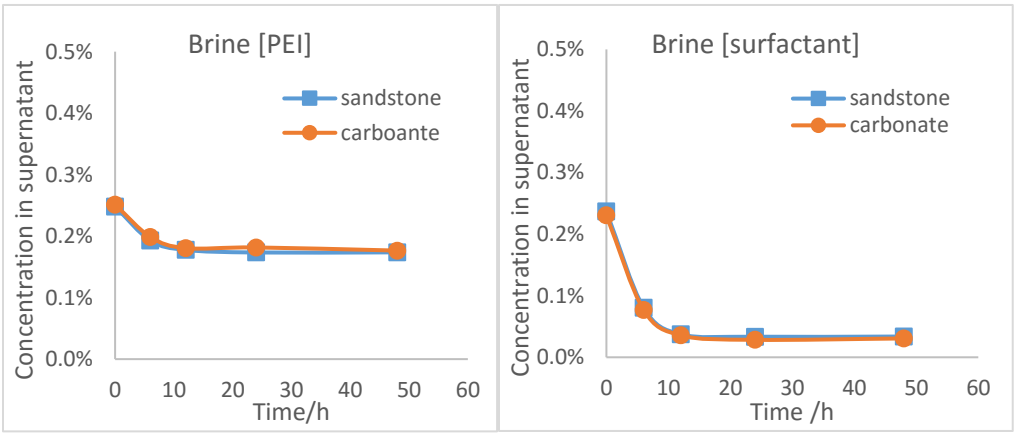

Figure 42 Comparison of surfactant and PEI adsorption in PEC suspension on sandstone and carbonate sand in (a) DI water and (b) brine

Adsorption of PEC on sandstone and carbonate sand were compared to study the effect of sand type. Results (Fig. 42) showed that carbonate sand accelerates the adsorption of PEC compared to sandstone in DI water whereas in brine both sand types yield the same PEC adsorption rate. For PEC adsorption in DI water, a slight difference between sandstone

and carbonate sand was observed and the adsorption rate on sandstone was a little slower than that on carbonate sand (Fig.42 (a)). Meanwhile they both had a tendency to reach the same eventual equilibrium concentration. Sandstone, mainly consisting of quartz, is much less soluble in DI water than carbonate, mainly composed of calcite and magnesite (Crain's petrophysicsal handbook January,2015). When PEC suspension was agitated with carbonate, a small amount of dissolved ions (Ca^{2+} and Mg^{2+}) from carbonate sand may accelerate PEC adsorption like salinity effect. Whereas the effect of the dissolved ions is very small due to the low solubility of carbonate. On the contrary, in terms of PEC adsorption in brine, the adsorption on two types of sands were same (Fig.42 (b)). The reason may be that the effect of brine is much stronger than the effect of dissolved ions from carbonate sand and thus PEC adsorption rate is mainly determined by the electrolyte from brine not the dissolved ions. Thus PEC adsorption on two different sands were similar. More experiments may be required to prove the above hypothetical explanation.

5.2.2 Real-time adsorption study by QCM-D

QCM-D instrument was used to monitor the real-time adsorption of surfactant and PEC in DI water on silicon sensor. The characteristics of real-time adsorption are indirectly reflected by the shift of frequency and dissipation. Frequency shift will decrease when materials are adsorbed onto the surface of sensors and with more materials adsorbed onto sensors frequency shift will become smaller. The rigidity of layers can be estimated from the shift of dissipation. When dissipation shift is close to zero or less than 5% of frequency shift and the dissipations shift from different overtones overlap with each other, the film can be treated as rigid film. Otherwise the film is considered as viscoelastic soft film.

5.2.2.1 Real-time adsorption of surfactant

(a)

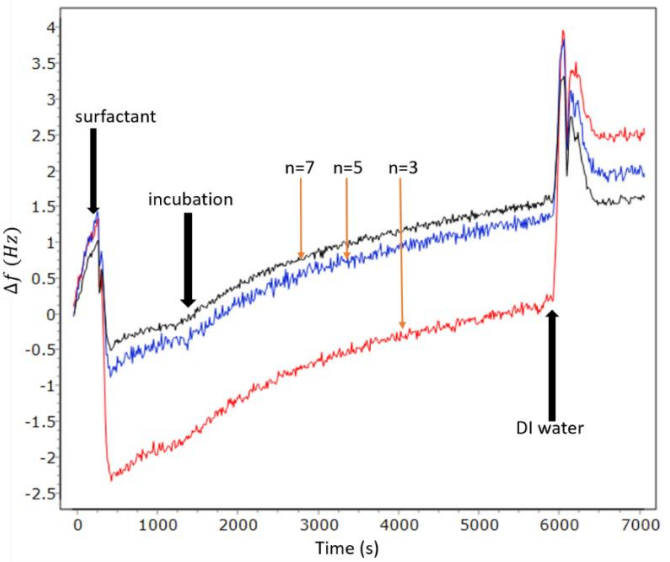

(b)

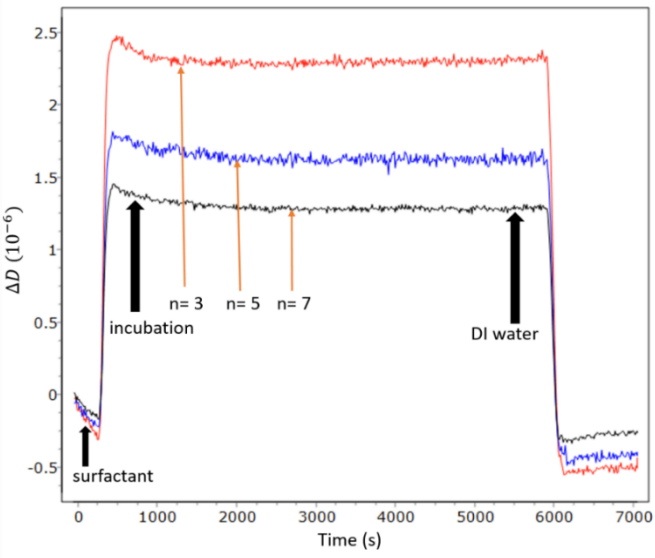

Figure 43 (a) Frequency raw data (Δf) and (b) dissipation raw data (ΔD) of sulfate surfactant real-time adsorption on silicon sensor in DI water. Δf and ΔD are measured simultaneously at three different overtones (n=3, 5, and 7)

To monitor the real-time adsorption of sulfate surfactant on silicon sensor, the sensor was firstly flushed by DI water, followed by surfactant and incubation, and then rinsed by DI water. QCM-D raw data (shown in Fig.43) illustrated that after the injection of surfactant, a small decrease of frequency shift and a relative large increase of dissipation shift were detected. During the incubation time, frequency shift kept increasing and went back to baseline. A decrease of frequency shift and a significant increase of dissipation shift during surfactant flushing period is explained by the formation of viscoelastic surfactant double layer. Sulfate surfactant (-) was not adsorbed strongly on the silicon sensor (-) due to the electrostatic repulsion between same charged silicon sensor and sulfate surfactant. Thus, surfactant desorbed from surface during incubation and frequency shift rose back to baseline. The results of real-time sulfate surfactant adsorption agreed well with static adsorption test on sand grains (see Fig.31) where the concentration of adsorbed surfactant was not detected.

5.2.2.2 Real-time adsorption of PEC

The proposed PEC adsorption model was tested by monitoring PEC real-time adsorption in DI water using QCM-D and silicon sensor. Raw data of PEC real-time adsorption are shown in Fig. 44.

(a)

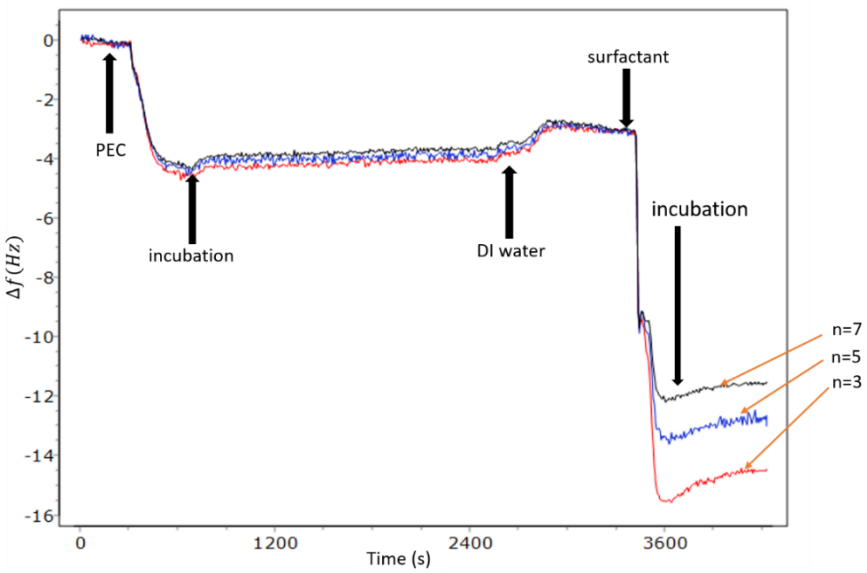

(b)

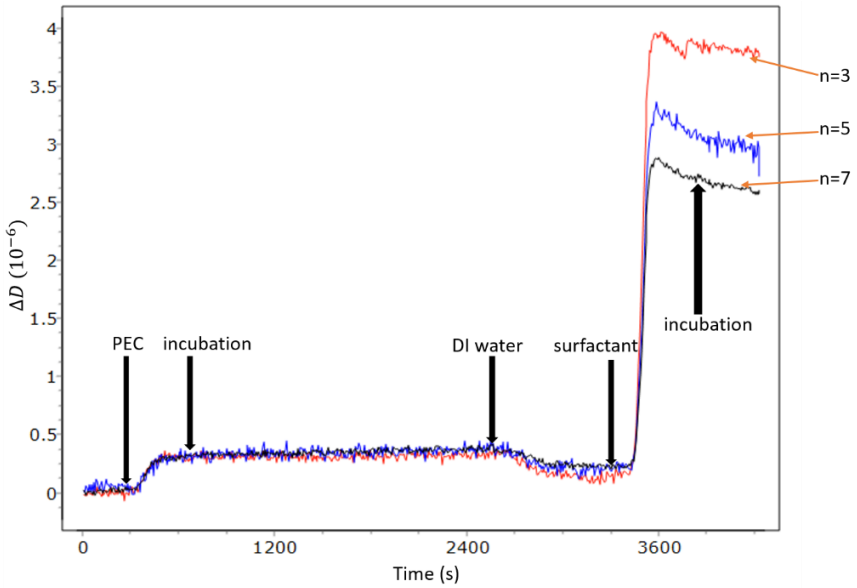

Figure 44 (a) Frequency raw data (Δf) and (b) dissipation raw data (ΔD) of PEC real-time adsorption on silicon sensor in DI water. Δf and ΔD are measured simultaneously at three different overtones (n=3, 5, and 7)

Experiment started with DI water flushing to build up a baseline. Next, the silicon sensor was flushed and incubated by PEC suspension, rinsed by DI water and then rinsed and

incubated by surfactant solution (Fig. 44). During PEC flushing period, a decrease of frequency shift and a relative small increase of overlapping dissipation shift were detected. This process corresponded to the adsorption of materials on the silicon sensor (-). A large amount of the PEC (+) and a small amount of free PEI (+) were firstly adsorbed on the oppositely charged silicon sensor (-) due to the electrostatic attraction. The adsorbates formed condense and rigid layer on the surface of silicon sensor leading to low and overlapping dissipation shift. Next, DI water was pumped to rinse the sensor and remove loosely adsorbed materials until the shift of frequency and dissipation went back to equilibrium. A relatively small shift of frequency and dissipation (see Fig.44) was observed because the strong electrostatic attraction between the opposite charged PEC/PEI (+) and silicon sensor (-) enabled adsorbates difficult to be flushed away. During the surfactant flushing period, 0.5% of sulfate surfactant was pumped to the silicon sensor. Frequency value exhibited significant shift compared to sulfate surfactant real-time adsorption data (Fig.43) and during incubation frequency shift remained almost unchanged. The significant shift of frequency and dissipation value resulted from the strong adsorption of surfactant (-) on the PEC/PEI (+) coated silicon sensor and the viscoelastic property of the formed surfactant double layer. Sulfate surfactant was adsorbed on the PEC/PEI coated surface due to the electrostatic force. The hydrophobic force between surfactants also enables the formation of a relative soft and viscoelastic surfactant layer. Real-time adsorption results of surfactant and PEC suspension obtained from QCM-D agreed well with the proposed PEC adsorption model.

CHAPTER VI

CONCLUSIONS

6.1 Bulk properties of PEC

Particle size and zeta potential of PEC largely depend on the parameters of preparation protocols including surfactant/PEI concentrations, surfactant to PEI weight ratio, and pH of PEI. With the increase of surfactant to PEI weight ratio, zeta potential decreases and particle size increases. That is primarily because positive charges on PEI are compensated by more negative charges from surfactant with the increasing surfactant amount in the system. The decreased zeta potential then reduces the repulsion force between charged PECs and leads to a larger particle size. In addition, positive charge density on PEI decreases with the increasing pH because of the nature of weak polyelectrolytes. Therefore, higher pH of PEI leads to lower zeta potential and larger particle size of PEC. A stable positively charged PEC system made from the preparation protocol of 1% sulfate surfactant: 1% PEI (pH=7) =1:1 was selected for further studies.

The stability test of PEC showed that PEC started to aggregate when sodium chloride concentration reached 7.5%. The addition of electrolyte screens out charged particles and reduces the zeta potential of PEC to a point which the repulsion force between PECs is unable to stabilize the colloidal system thus aggregations appear.

The surfactant entrapment efficiency (EE) of the prepared PEC is about 75% obtained by MB titration method. In addition, MB titration method showed that the addition of sodium carbonate powders released surfactant from PEC by changing the charge density on PEI.

6.2 Adsorption study of PEC

A TOC/TN analytical method was developed and used to measure the concentrations of sulfate surfactant and PEI in PEC suspension before and after the PEC static adsorption test.

Both static adsorption using sand grains and real-time adsorption using silica sensor showed that only little anionic sulfate surfactants would be adsorbed by the negatively charged surfaces. On the contrary, a large adsorption of sulfate surfactant entrapped in the PEC static adsorption test was observed.

Results from both static adsorption and real-time adsorption by QCM-D showed that PEC coated negatively charged sandstone grains and silicon sensors were more likely to adsorb the anionic surfactant than those without PEC treatment.

Based on the observations of static and real-time adsorption of PEC suspension, PEC adsorption model was proposed and confirmed. When PEC suspension is agitated with negatively charged sand grains, PEC (+) and free PEI (+) will be firstly adsorbed onto the sand surface (-) to form the first layer and then free anionic surfactant (-) will be adsorbed to the PEC/PEI coated surface (+). According to this model, the wettability of rock surface may be changed by surfactant entrapped in PEC system through the amphiphilic properties of the surfactants adsorbed on the rock surface.

The effect of electrolyte and sand type on PEC adsorption were investigated. It is found that it takes less time for PEC to be adsorbed in brine than in DI water. This can be

explained by the DLVO theory where electrolyte reduces the repulsion force and energy barrier between adsorbed PECs thus promotes PEC adsorption rate.

The adsorption rate of PEC is faster with carbonate sand than sandstone in DI water while this effect was not significant in brines. The faster adsorption on carbonate sand in DI water may be explained by the effect of dissolved ions from carbonates. But in brines, the existing ions were much more than the dissolved ions from carbonates and control the PEC adsorption on sands. Therefore, similar adsorption rate on both carbonate sand and sandstone in brines was observed. More experiments may be required to prove the above hypothetical explanation.

REFERENCES

Agenet, N., et al. (2012). Fluorescent Nanobeads: a First Step Toward Intelligent Water Tracers, Society of Petroleum Engineers.

Bain, C. D., et al. (2010). "Complexes of surfactants with oppositely charged polymers at surfaces and in bulk." Advances in Colloid and Interface Science **155**(1–2): 32-49.

Baskaralingam, P., et al. (2006). "Adsorption of acid dye onto organobentonite." Journal of Hazardous Materials **128**(2–3): 138-144.

Bennetzen, M. V. and K. Mogensen (2014). Novel Applications of Nanoparticles for Future Enhanced Oil Recovery, International Petroleum Technology Conference.

Biswas, S. C. and D. K. Chattoraj (1998). "Kinetics of Adsorption of Cationic Surfactants at Silica-Water Interface." Journal of Colloid and Interface Science **205**(1): 12-20.

Boussif, O., et al. (1995). "A versatile vector for gene and oligonucleotide transfer into cells in culture and in vivo: polyethylenimine." Proceedings of the National Academy of Sciences of the United States of America **92**(16): 7297-7301.

Brenner, T., et al. (2012). "Adsorption of nanoparticles at the solid–liquid interface." Journal of Colloid and Interface Science **374**(1): 287-290.

Brookhaven Instrument Corporation. NanoBrook Omni Particle Sizer and Zeta Potential analyzer.

Crain's petrophysicsal handbook (January,2015). "Carbonate versus sandstone reservoirs." Retrieved June,1, 2016, from https://www.spec2000.net/17-speccarb.htm.

Cordova, M., et al. (2008). "Delayed HPAM Gelation via Transient Sequestration of Chromium in Polyelectrolyte Complex Nanoparticles." Macromolecules 41(12): 4398-4404.

Gao, B. and M. M. Sharma (2012). A New Family of Anionic Surfactants for EOR Applications, Society of Petroleum Engineers.

Gao, Y. (2014). Fundamental Studies of Refined Polyelectrolyte/Surfactant Nanoparticles Bulk and Interfical Properties. Department of Chemical and Petroleum Engineering University of Kansas. **PHD**.

Gao, Y., et al. (2013). "Interface-Induced Disassembly of a Self-Assembled Two-Component Nanoparticle System." Langmuir **29**(11): 3654-3661.

Ghosh, P. DLVO Theory and Non-DLVO Forces, Department of Chemical Engineering, NPTEL. **Module 3, Lecture 5**.

Hendraningrat, L., et al. (2012). A Glass Micromodel Experimental Study of Hydrophilic Nanoparticles Retention for EOR Project (Russian), Society of Petroleum Engineers.

Hoelscher, K. P., et al. (2012). Application of Nanotechnology in Drilling Fluids, Society of Petroleum Engineers.

Jurado, E., et al. (2006). "Simplified spectrophotometric method using methylene blue for determining anionic surfactants: Applications to the study of primary biodegradation in aerobic screening tests." Chemosphere **65**(2): 278-285.

Karnel R. Walker, L. S., and Robert H. Clifford Total Nitrogen Analysis: A New Perspective on TOC.

Kwok, W., et al. (1993). "Static and dynamic adsorption of a non-ionic surfactant on Berea sandstone." Colloids and Surfaces A: Physicochemical and Engineering Aspects **78**: 193-209.

L.Schramm, L. (2000). Surfactants: Fundamentals and applications in the petroleum industry, cambridge university press.

Lankalapalli, S. and V. R. M. Kolapalli (2009). "Polyelectrolyte Complexes: A Review of their Applicability in Drug Delivery Technology." Indian Journal of Pharmaceutical Sciences **71**(5): 481-487.

Levitt, D., et al. (2009). "Identification and Evaluation of High-Performance EOR Surfactants."

Li, Y. V. and L. M. Cathles (2014). "Retention of silica nanoparticles on calcium carbonate sands immersed in electrolyte solutions." Journal of Colloid and Interface Science **436**: 1-8.

Lv, W., et al. (2011). "Static and dynamic adsorption of anionic and amphoteric surfactants with and without the presence of alkali." Journal of Petroleum Science and Engineering **77**(2): 209-218.

Malvern Instrument Application Note: Measuring zeta potential using phase analysis light scattering (PALS), Malvern Instrument.

Mezei, A., et al. (2007). "Effect of Mixing on the Formation of Complexes of Hyperbranched Cationic Polyelectrolytes and Anionic Surfactants." Langmuir **23**(8): 4237-4247.

Mezei, A., et al. (2008). "Nonequilibrium Features of the Association between Poly(vinylamine) and Sodium Dodecyl Sulfate: The Validity of the Colloid Dispersion Concept." The Journal of Physical Chemistry B **112**(32): 9693-9699.

Müller, M., et al. (2005). "Needlelike and Spherical Polyelectrolyte Complex Nanoparticles of Poly(l-lysine) and Copolymers of Maleic Acid." Langmuir **21**(1): 465-469.

Naderi, A., et al. (2005). "Trapped non-equilibrium states in aqueous solutions of oppositely charged polyelectrolytes and surfactants: effects of mixing protocol and salt concentration." Colloids and Surfaces A: Physicochemical and Engineering Aspects **253**(1–3): 83-93.

Nevskaia, D. M., et al. (1998). "Adsorption of Polyoxyethylenic Nonionic and Anionic Surfactants from Aqueous Solution: Effects Induced by the Addition of NaCl and CaCl2." Journal of Colloid and Interface Science **205**(1): 97-105.

Nylander, T., et al. (2006). "Formation of polyelectrolyte–surfactant complexes on surfaces." Advances in Colloid and Interface Science **123–126**: 105-123.

Ogolo, N. A., et al. (2012). Enhanced Oil Recovery Using Nanoparticles, Society of Petroleum Engineers.

Ondaral, S., et al. (2010). "Surface-Induced Rearrangement of Polyelectrolyte Complexes: Influence of Complex Composition on Adsorbed Layer Properties." Langmuir **26**(18): 14606-14614.

Onyekonwu, M. O. and N. A. Ogolo (2010). Investigating the Use of Nanoparticles in Enhancing Oil Recovery, Society of Petroleum Engineers.

Paria, S. and K. C. Khilar (2004). "A review on experimental studies of surfactant adsorption at the hydrophilic solid–water interface." Advances in Colloid and Interface Science **110**(3): 75-95.

Pokrovsky, O. S., et al. (1999). "Dolomite surface speciation and reactivity in aquatic systems." Geochimica et Cosmochimica Acta **63**(19–20): 3133-3143.

Q-Sense Company. Quartz Crystal Microbalance With Dissipation (QCM-D).

Q-Sense Company. Technology Note: study of viscoelastic films – a comparison between the Voigt viscoelastic model and the Sauerbrey relation, Q-Sense Company.

Ragab, A. M. S. and A. E. Hannora (2015). An Experimental Investigation of Silica Nano Particles for Enhanced Oil Recovery Applications, Society of Petroleum Engineers.

Reihs, T., et al. (2003). "Deposition of polylelectrolyte complex nano-particles at silica surfaces characterized by ATR-FTIR and SEM." Colloids and Surfaces A: Physicochemical and Engineering Aspects **212**(1): 79-95.

Reihs, T., et al. (2004). "Preparation and adsorption of refined polyelectrolyte complex nanoparticles." Journal of Colloid and Interface Science **271**(1): 69-79.

Rezvani Amin, Z., et al. (2013). "The Effect of Cationic Charge Density Change on Transfection Efficiency of Polyethylenimine." Iranian Journal of Basic Medical Sciences **16**(2): 150-156.

Robertson, A. P. and J. O. Leckie (1997). "Cation Binding Predictions of Surface Complexation Models: Effects of pH, Ionic Strength, Cation Loading, Surface Complex, and Model Fit." Journal of Colloid and Interface Science **188**(2): 444-472.

Rosen, M. J. (2004). surfactant and interficial phenomena, A JOHN WILEY & SONS, INC., PUBLICATION.

S.R.Epton (December, 6, 1947). "A Rapid Method of Analysis for Certain Surface-Active Agents." Nature **160**(4075): 795-796.

Sandersen, S. B. (2012). Enhanced Oil Recovery with Surfactant Flooding. Department of Chemical and Biochemical Engineering, Technical University of Denmark. **PHD**.

Santra, A. K., et al. (2012). Influence of Nanomaterials in Oilwell Cement Hydration and Mechanical Properties, Society of Petroleum Engineers.

Sean X. Liu, J.-T. K. (August, 2009). "Application of Kevin—Voigt Model in Quantifying Whey Protein Adsorption on Polyethersulfone Using QCM-D." JALA **01**(003).

Shimadzu Company (July, 2013). Total Organic Carbon Analyzer TOC-L CPH/CPN User's Manual**:** 330-334.

Soft Matter Wiki. "DLVO theory." Retrieved 16 May, 2016, from http://soft-matter.seas.harvard.edu/index.php/DLVO_theory.

Solomatin, S. V., et al. (2003). "Environmentally Responsive Nanoparticles from Block Ionomer Complexes: Effects of pH and Ionic Strength." Langmuir **19**(19): 8069-8076.

Somasundaran, P. and L. Zhang (2006). "Adsorption of surfactants on minerals for wettability control in improved oil recovery processes." Journal of Petroleum Science and Engineering **52**(1–4): 198-212.

Wang, Y., et al. (2011). "Surfactant induced reservoir wettability alteration: Recent theoretical and experimental advances in enhanced oil recovery." Petroleum Science **8**(4): 463-476.

Yanez Arteta, M., et al. (2013). "Interactions of PAMAM Dendrimers with SDS at the Solid–Liquid Interface." Langmuir **29**(19): 5817-5831.

Yu, J., et al. (2010). Transport Study of Nanoparticles for Oilfield Application, Society of Petroleum Engineers.